ISLAMIC UNIVERSITY OF TECHNOLOGY (IUT)

DYNAMIC MODELING AND CONTROL OF PERMANENT MAGNET SYNCHRONOUS GENERATOR (PMSG) IN WIND ENERGY CONVERSION SYSTEM

BY

A. K. M .SIFAT HAIDER
SHOWROV RAHMAN
NURUL AMBIA ALAUL

A Dissertation
Submitted in Partial Fulfillment of the Requirement for the
Bachelor of Science in Electrical and Electronic Engineering
Academic Year: 2014-2015

Department of Electrical and Electronic Engineering.
Islamic University of Technology (IUT)
A Subsidiary Organ of OIC
Dhaka, Bangladesh.

A Dissertation on

DYNAMIC MODELING AND CONTROL OF PERMANENT MAGNET SYNCHRONOUS GENERATOR (PMSG) IN WIND ENERGY CONVERSION SYSTEM

Submitted by

SHOWROV RAHMAN **A. K. M. SIFAT HAIDER** **NURUL AMBIA ALAUL**

Approved By

PROF. DR. MD. SHAHID ULLAH

Head of the Department
Department of Electrical and Electronic Engineering
Islamic University of Technology (IUT)
Gazipur-1704, Bangladesh.

Supervised by

ASHIK AHMED

Assistant Professor
Department of Electrical and Electronic Engineering
Islamic University of Technology (IUT)

Contents:

To our beloved parents

Abstract

Because of the scarcity of available energy resources, it is a matter of time that we have to depend on renewable energy in the near future. And in that case wind energy has to play an important role. But one problem is that wind availability is sporadic and unpredictable and wind speed varies time to time. In response to that problem effective designing of the controller parameters of a direct drive permanent magnet synchronous generator (PMSG) connected to power grid is proposed in this thesis.

In our proposed model the direct drive PMSG is connected to the grid network through a back to back full scale converter, coupling transformer and a Low Pass Filter (LPF).

Eigen value analysis is used to analyze the small signal stability of the system and the parameters of the system can be well chosen by means of Eigen values sensitive analysis. The relation between modes and state variables can be discovered. Then the influences of the controller's parameters on the traces of Eigen values are analyzed. According to the traces of Eigen values controller's parameters and verification of the system stability under some parameter variations were achieved.

The simulation results show that with optimized controller parameters the system stability is improved after suffering disturbance of a wind velocity variation and the system dynamic response is consistent with the result of a small signal analysis.

Keyword: Permanent Magnet Synchronous generator, Eigen Value, linearization, Initialization, Nonlinear modeling, Small signal modeling, Stability.

Acknowledgements

This work has been carried out at the Renewable energy sector, Department of Electrical and Electronic Engineering at Islamic University of Technology (IUT) an organization of OIC, Prof. Dr. Md. Shahid Ullah, Head of the department (EEE) is gratefully acknowledged.

First of all, we would like to express my deep and sincere gratitude to our supervisor Assistant Professor Ashik Ahmed for his excellent supervision and helps during this work.

We would like to express gratitude to all my Professors for providing guidance and encouragement and valuable suggestions and constructive advice on this thesis.

Our heartiest gratitude to our batch mates and all the faculty members of the EEE department IUT.

Engineering and the Experimental equipment's provided by IUT authority is providing such a nice atmosphere.

Our ultimate gratitude goes to our parents, brothers, sisters, relatives and our beloved ones. It is because of their endless pray, finally we can accomplish this work.

Thank you for your love, which makes this work so joyful.

Chapter 1

Introduction

1.1 Renewable energy

The energy sources which are naturally renewed with time is called renewable energy. The supply of this energy doesn't depend upon the rate of consumption. It is environmentally friendly. It is green energy promoted by state and GEF fund and in accordance with other UN resolutions.

Our resources are decreasing day by day. Someday we should depend totally on our nature. In the matter of fact that renewable energy sources are used rapidly nowadays to meet the demand and available in the scarcity of fossil fuels. Renewable energy resources exist over wide geographical areas, in contrast to other energy sources, which are concentrated in a limited number of countries. Rapid deployment of renewable energy and energy efficiency is resulting in significant energy security, climate change mitigation, and economic benefits. At the national level, at least 30 nations around the world already have renewable energy contributing more than 20 percent of energy supply. National renewable energy markets are projected to continue to grow strongly in the coming decade and beyond. While many renewable energy projects are large-scale, renewable technologies are also suited to rural and remote areas and developing countries, where energy is often crucial in human development. United Nations' Secretary-General Ban Ki-moon has said that renewable energy has the ability to lift the poorest nations to new levels of prosperity [1]. Renewable energy resources and significant opportunities for energy efficiency exist over wide geographical areas, in contrast to other energy sources, which are concentrated in a limited number of countries. It would also reduce environmental pollution such as air pollution caused by burning of fossil fuels and improve public health. From the end of 2004, worldwide renewable energy capacity grew at rates of 10–60% annually for many technologies. There are different types of renewable energy sources. These are:

- Wind energy
- Hydro energy
- Solar energy
- Geothermal energy
- Bio energy

1.2 Wind energy

Using the flow of wind, the generation of electricity is occurred. The movement of the atmosphere is driven by differences of temperature at the Earth's surface due to varying temperatures of the Earth's surface when lit by sunlight. Wind energy can be used to pump

water or generate electricity. Globally, the long-term technical potential of wind energy is believed to be five times total current global energy production, or 40 times current electricity demand, assuming all practical barriers needed were overcome. This would require wind turbines to be installed over large areas, particularly in areas of higher wind resources, such as offshore. As offshore wind speeds average ~90% greater than that of land, so offshore resources can contribute substantially more energy than land stationed turbines [2]. It is most expanding renewable energy source. It is the use of kinetic energy of wind. More wind power capacity was added during 2009 than any other renewable technology.

1.2.1 Importance of wind energy

- Wind is free.
- No emission of greenhouse gases.
- Scarce resources of fossil fuel
- Low installment and maintenance cost.
- Although wind turbines can be very tall each takes up only a small plot of land. This means that the land below can still be used. This is especially the case in agricultural areas as farming can still continue.
- Remote areas that are not connected to the electricity power grid can use wind turbines to produce their own supply.
- Wind turbines are available in a range of sizes.

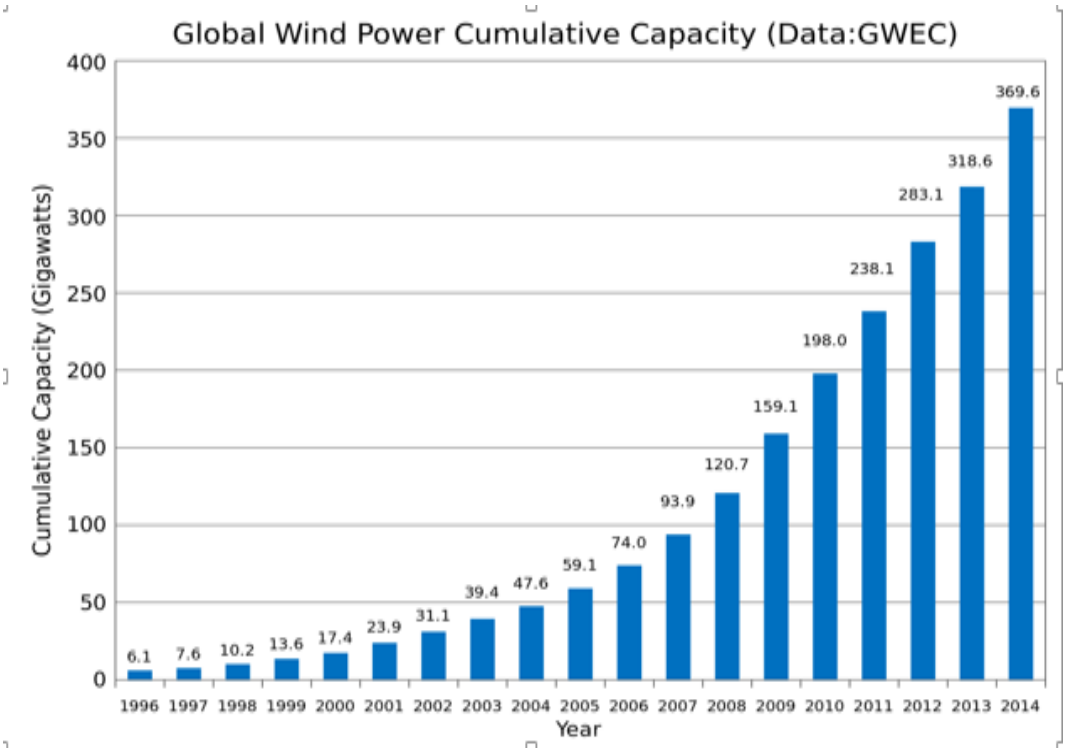

Fig 1.1: Global wind power generation throughout the years. [13]

1.2.2 Interesting wind energy facts

- Wind mills have been in use since 2000 B.C. and were first developed in China and Persia.
- Wind power is currently the fastest growing source of electricity production in the world.
- A single wind turbine can power 500 homes.
- In 2013, the roughly 168 million megawatt-hours generated by wind energy avoided 95.6 million metric tons of CO_2 –the equivalent of reducing power sector CO_2 emissions by 4.4% or removing 16.9 million cars from the roads.
- Most wind turbines (95%) are installed in private land**.**
- Modern wind turbines produce 15 times more electricity than the typical turbine did in 1990/
- Unlike nearly every other form of energy, wind power uses virtually no water [3]

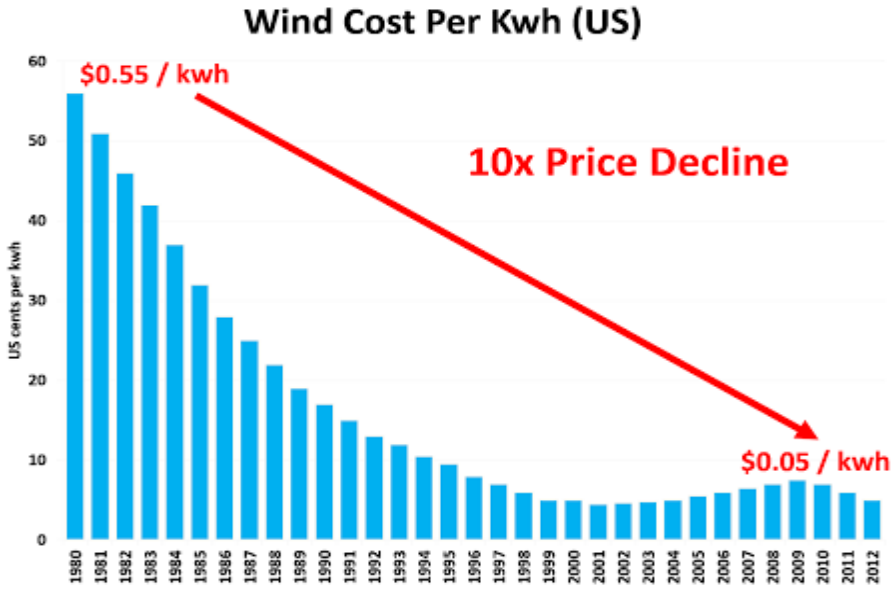

Fig 1.2: Decreasing rate of wind cost throughout the years. [13]

1.3 Prospects of Bangladesh

Bangladesh is supposed to have a huge demand of 10283 MW by the end of the year 2015;of which only a negligible 100MW is projected to be generated from the wind source. The country has 724km of coastline area which experiences sea-breeze blow in the summer months. The goal of this study is to analyze the feasibility of installing different levels of wind turbines in Bangladesh and for this purpose wind speed data for years 2002-2011 is taken into consideration. The whole country is divided into 7 sectors each having at least 2 samples making a total of 35 samples. From these samples Wind Power Density (WPD) of the different places are calculated at 50m and 120m height. Plant capacity factor (PCF) is calculated from the generated output power calculated by using MATLAB. Then they are categorized into

different power classes. Based on these power classes different scales of generation are assigned to different places. In this process other factors like Availability of Wind, Average Monthly Wind Speed, and Average Yearly Wind Speed are taken into consideration. All 35 places fall in power class 1 at 50m height. At 120m height Chittagong and Jessore fall in power class 5, Khepupara in class 3, Cox's Bazar and Hatiya in class 2 and rest of the places in power class 1 at 120m height. Other 30 places fall into power class 1. At 120m height large scale generation is possible at Chittagong and Jessore, medium scale at Khepupara and small scale at Cox's Bazar and Hatiya. And the rest 30 places still remain suitable for micro scale generation. Chittagong has a good PCF in the range of 33% to 85% throughout the year; July has the highest PCF with 85%.So a decent amount of power can be generated by using wind energy from these places.

The potential of wind energy is limited to coastal areas, off-shore islands, rivers sides and other inland open areas with strong wind regime. In order to generate electricity from Wind Energy, BPDB installed 4x225 KW = 900 KW capacity grid connected Wind Plant at Muhuri Dam area of Sonagazi in Feni.

Another project of 1000 KW Wind Battery Hybrid Power Plant at Kutubdia Island was completed in 2008 which consists of 50 Wind Turbines of 20 kW capacity each.

1.4 Objective of this thesis

In [5], by introducing of a frequency deviation signal into the control system, an improved pitch control scheme was presented. In [6], a new performance robustness criterion for performance evaluation was proposed. In [6-12], the small signal stability of doubly-fed induction generator (DFIG)-based wind power system was analyzed and optimization of controller to enhance small signal stability was performed. In [12], the impacts of the rotor current controller parameters on the Eigen values traces study. In [13-14] analysis of small signal modeling of PMSG wind generation. Above mentioned references focused on the small signal modelling and analysis of squirrel cage induction generator and DFIG The small signal modeling and analysis of PMSG wind generation system has been seldom researched. In [13-14], the small signal stability of PMSG wind generation system is analyzed but they did not design the control system according to Eigen value method. Small signal modelling of wind turbine with direct-drive PMSG connected to power grid. Verification of the system stability under some parameter variations according to the traces of eigenvalues. Enhancement of system stability by optimization of controller parameters is our main objective of this thesis.

Chapter 2

Wind energy system

2.1 Wind power generation from wind

The amount of the kinetic energy in the air flow can be determined based on the size of wind turbine and the wind speed. The elementary momentum theory gives an explanation of energy conversion in ideal circumstances. The amount of the kinetic energy of a fluid mass m with a mass density ρ, moving at a velocity ϑ through the area A is

$$E = \frac{1}{2}.m.\vartheta^2 \qquad (2.1)$$

And the mass flow is

$$m = A.\rho.\vartheta \qquad (2.2)$$

The power available in the wind is equal to the amount of energy yield passing per second

$$P_{wind} = E.m = \frac{1}{2}.\rho.A.\vartheta^3 \qquad (2.3)$$

It is obvious that a small variation in the wind speed influences the available wind power drastically. It was first in 1922, the German engineer Betz showed that the amount of extractable energy from an air stream is limited. It was shown that, in a free air stream, the maximum energy is extracted if the wind speed is reduced by three times far behind the turbine in comparison to in front of it. The maximum extractable power becomes then, 16/27 of available wind power [4]. As mentioned, it is not possible to capture all the power in the air flow as this would result in air standstill immediately after the wind turbine. Aerodynamic efficiency represents a ratio of captured power and available wind power. In wind power terminology, it is more known as the power coefficient. Betz factor is the maximum value for the power coefficient. The power coefficient C_p is a function of the tip speed ratio γ and the blade pitch angle β. So above equation can be modified as

$$P_{mech} = C_p.P_{wind} = \frac{1}{2}.\rho.A.C_p(\gamma,\beta).\vartheta^3 \qquad (2.4)$$

Where

$$\gamma = \frac{r.\omega}{\vartheta} \qquad (2.5)$$

ω is the rotor tip angular speed and r is the rotor plane radius. Blade pitching means that the rotor blades are rotated along their axis, in order to control the amount of the absorbed power. In wind turbines which are not equipped with the control of the blade pitch, power coefficient

is merely function of the tip speed ratio. The rotor power coefficient as a function of tip speed ratio and pitch angle is shown in Figure 2.1

Power coefficient is maximum at the optimum tip speed ratio i.e. in order to capture the maximum energy, the wind turbine rotor has to be run at this ratio. When the wind turbine rotor is run at other tip speed ratios, eddies will develop at the blade tip. This phenomenon reduces the captured energy and it is called stall. It explains the drop of the power coefficient at other tip speed ratios. It can be observed from the power coefficient diagram that the wind turbine is not self-starting. For low values of the tip speed ratio, the value of the power coefficient is negative. Many lift based wind turbines require a minimum tip speed ratio before they can start to absorb the power [5]. Accordingly, in order to start up the wind turbine rotor, energy has to be supplied. There are different ways to do so, one is to utilize an auxiliary self-starting turbine like for example Savonious wind turbine. Another is certain modification in the design of the wind turbine. Furthermore, electrical starting of wind turbine is yet another possibility. The generator is, then, fed by the grid for a short duration of time and works as a motor in order to start the wind turbine. In this solution the wind power plant cannot operate as a stand-alone unit.

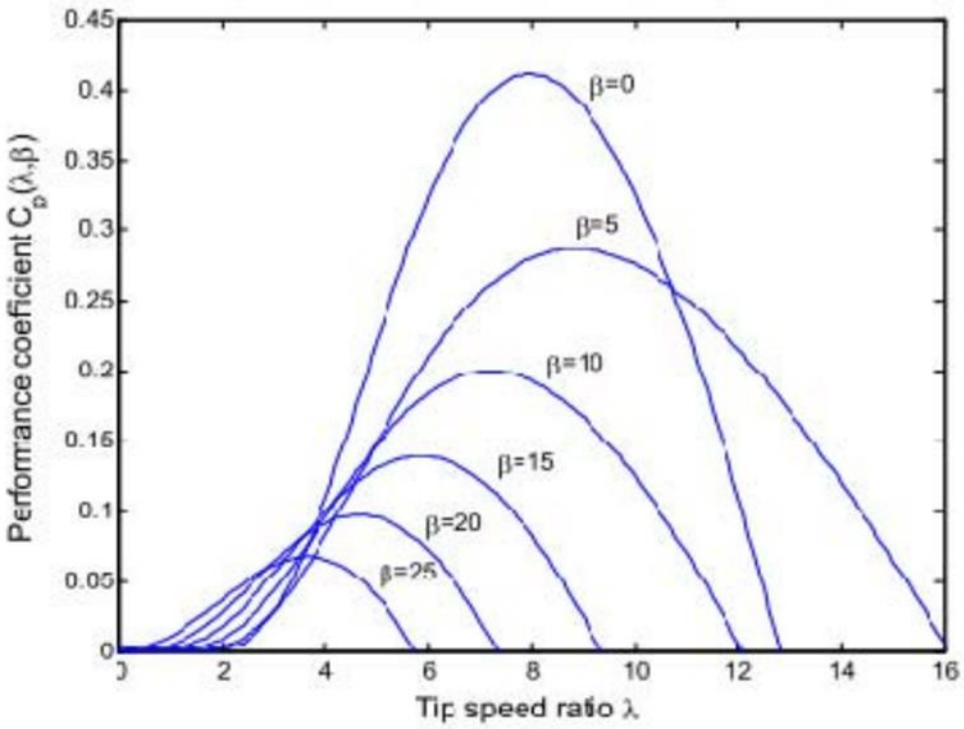

Figure 2.1: Power coefficient as function of γ and β

2.2 Wind turbine and its classifications

A wind turbine is a device that converts kinetic energy from the wind into electrical power. The term appears to have migrated from parallel hydroelectric technology (rotary propeller). The technical description for this type of machine is an aero foil-powered generator.

Types of wind turbine:

Wind turbines are categorized based on two different criteria,

a) First due to their aerodynamic function
b) Second based on their design.

Considering the aerodynamic performance, wind turbines are divided into drag based and lift based.

Drag based/low speed:

The rotors which utilize the drag force of the wind are recognized as low speed turbines.

Lift based:

The lift based turbines are recognized as high speed rotors. These are capable of capturing higher amount of the wind power compared to their drag based counterparts.

Due to the second criterion, wind turbines are classified based on their axis of rotation.

Horizontal Axis Wind Turbines (HAWT):

Horizontal-axis wind turbines (HAWT) have the main rotor shaft and electrical generator at the top of a tower, and must be pointed into the wind. Small turbines are pointed by a simple wind vane, while large turbines generally use a wind sensor coupled with a servo motor. Most have a gearbox, which turns the slow rotation of the blades into a quicker rotation that is more suitable to drive an electrical generator.

Since a tower produces turbulence behind it, the turbine is usually positioned upwind of its supporting tower. Turbine blades are made stiff to prevent the blades from being pushed into the tower by high winds. Additionally, the blades are placed a considerable distance in front of the tower and are sometimes tilted forward into the wind a small amount.

Downwind machines have been built, despite the problem of turbulence (mast wake), because they don't need an additional mechanism for keeping them in line with the wind, and because in high winds the blades can be allowed to bend which reduces their swept area and thus their wind resistance. Since cyclical (that is repetitive) turbulence may lead to fatigue failures, most HAWTs are of upwind design.

Turbines used in wind farms for commercial production of electric power are usually three-bladed and pointed into the wind by computer-controlled motors. These have high tip speeds of over 320 km/h (200 mph), high efficiency, and low torque ripple, which contribute to good reliability. The blades are usually colored white for daytime visibility by aircraft and range in

length from 20 to 40 meters (66 to 131 ft.) or more. The tubular steel towers range from 60 to 90 meters (200 to 300 ft.) tall. The blades rotate at 10 to 22 revolutions per minute. At 22 rotations per minute the tip speed exceeds 90 meters per second (300 ft./s). A gear box is commonly used for stepping up the speed of the generator, although designs may also use direct drive of an annular generator. Some models operate at constant speed, but more energy can be collected by variable-speed turbines which use a solid-state power converter to interface to the transmission system. All turbines are equipped with protective features to avoid damage at high wind speeds, by feathering the blades into the wind which ceases their rotation, supplemented by brakes. HAWT s have benefited from technological advancements in the aircraft engineering because of the blades' propeller like design. For instance, to achieve more lift forces, blade shapes' optimization are proposed and applied. Power coefficients up to 0.5 of HAWT s have been reported.

Vertical Axis Wind Turbines (VAWT):

Vertical-axis wind turbines (or VAWTs) have the main rotor shaft arranged vertically. One advantage of this arrangement is that the turbine does not need to be pointed into the wind to be effective, which is an advantage on a site where the wind direction is highly variable. It is also an advantage when the turbine is integrated into a building because it is inherently less steerable. Also, the generator and gearbox can be placed near the ground, using a direct drive from the rotor assembly to the ground-based gearbox, improving accessibility for maintenance.

The key disadvantages include the relatively low rotational speed with the consequential higher torque and hence higher cost of the drive train, the inherently lower power coefficient, the 360 degree rotation of the aero foil within the wind flow during each cycle and hence the highly dynamic loading on the blade, the pulsating torque generated by some rotor designs on the drive train, and the difficulty of modelling the wind flow accurately and hence the challenges of analyzing and designing the rotor prior to fabricating a prototype.

When a turbine is mounted on a rooftop the building generally redirects wind over the roof and this can double the wind speed at the turbine. If the height of a rooftop mounted turbine tower is approximately 50% of the building height it is near the optimum for maximum wind energy and minimum wind turbulence. Wind speeds within the built environment are generally much lower than at exposed rural sites, noise may be a concern and an existing structure may not adequately resist the additional stress. VAWT s have reached power coefficient up to 0.4 at maximum. Simplicity of the design of the VAWT s is beneficial.

In some of the researchers' opinion the VAWTs' power coefficient can exceed that of HAWTs'.

Figure 2.2 and Figure 2.3 show an H rotor VAWT and an installed HAWT respectively.

Fig 2.2: An H rotor (VAWT) [6].

Figure 2.3. A 450 kW HAWT with 37 m rotor diameter [4].

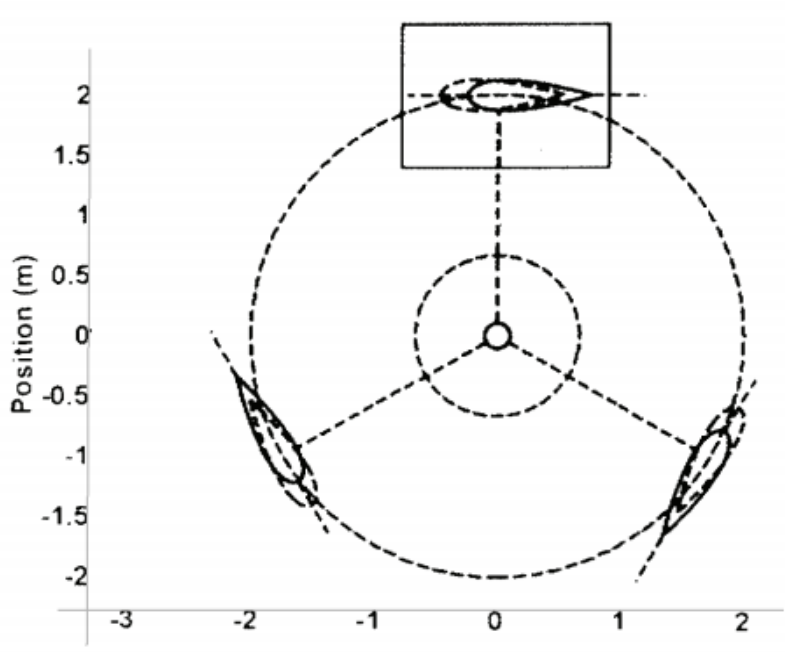

Figure 2.4. Horizontal plan of a VAWT [7].

2.3 Designing and construction:

Wind turbines are designed to exploit the wind energy that exists at a location. Aerodynamic modeling is used to determine the optimum tower height, control systems, number of blades and blade shape.

Wind turbines convert wind energy to electricity for distribution. Conventional horizontal axis turbines can be divided into three components:

- The rotor component, which is approximately 20% of the wind turbine cost, includes the blades for converting wind energy to low speed rotational energy.
- The generator component, which is approximately 34% of the wind turbine cost, includes the electrical generator, the control electronics, and most likely a gearbox (e.g. planetary gearbox), adjustable-speed drive or continuously variable transmission component for converting the low speed incoming rotation to high speed rotation suitable for generating electricity.
- The structural support component, which is approximately 15% of the wind turbine cost, includes the tower and rotor yaw mechanism.

A 1.5 MW wind turbine of a type frequently seen in the United States has a tower 80 meters (260 ft.) high. The rotor assembly (blades and hub) weighs 22,000 kilograms (48,000 lb.). The nacelle, which contains the generator component, weighs 52,000 kilograms (115,000 lb.). The concrete base for the tower is constructed using 26,000 kilograms (58,000 lb.) of reinforcing steel and contains 190 cubic meters (250 cu yd.) of concrete. The base is 15 meters (50 ft.) in diameter and 2.4 meters (8 ft.) thick near the center.

Among all renewable energy systems wind turbines have the highest effective intensity of power-harvesting surface because turbine blades not only harvest wind power, but also concentrate it.

Unconventional designing:

One E-66 wind turbine at Windpark Holtriem, Germany, carries an observation deck, open for visitors. Another turbine of the same type, with an observation deck, is located in Swaffham, England. Airborne wind turbines have been investigated many times but have yet to produce significant energy. Conceptually, wind turbines may also be used in conjunction with a large vertical solar updraft tower to extract the energy due to air heated by the sun.

Wind turbines which utilize the Magnus effect have been developed.

The ram air turbine is a specialist form of small turbine that is fitted to some aircraft. When deployed, the RAT is spun by the airstream going past the aircraft and can provide power for the most essential systems if there is a loss of all on–board electrical power.

2.4 Fixed Speed or Variable Speed wind turbine:

Fixed speed wind turbine

In fixed speed wind systems, the rotor speed is determined by the grid frequency and its variation is limited to around ±1% of the nominal speed. Usually, the fixed speed wind systems is designed in such a way that it has its optimum wind speed equal to site mean wind speed. No means for power control is applied and the advantage is simplicity of operation. Disadvantages are low efficiency of wind energy system in other wind conditions aside from the mean wind speed, and severe dynamics performance. Since no control method is implemented, any fluctuations of power i.e. disturbances in the grid and/or turbulence in the wind, are passed through the system without any damping. This reduces the quality of the delivered power to the grid and also causes mechanical stress on the wind turbine rotor. Weak power systems are sensitive to low power quality delivered by such wind systems.

The efficiency of electrical machines varies with varying electrical load conditions. Therefore most of the fixed speed wind energy systems are designed in a way to provide the generator with high load. This can be achieved by means of two generators with different ratings. Another solution is to have two windings with different pole numbers in the same generator.

Variable speed wind turbine

In Variable Speed wind systems, power electronics converters keeps the rotor speed and the grid frequency apart. Therefore it is possible to vary the rotor speed independent of the grid frequency. Hence, the variation in the input power will result in the rotor speed variation. The output power from wind system will be slightly lower than the input power which results in more stable and smooth delivered power to the grid. The power quality of these wind energy systems is much better compared to their fixed speed counterparts. Furthermore, they have lower noise in low wind conditions. In variable speed systems, the wind turbine is operated in a wider speed range, keeping the tip speed ratio at the optimum. The advantage is higher energy capture, however, the disadvantage is more complicated control method.

Chapter 3

Small signal modeling of the system

3.1 Small signal modeling

Small-signal modeling is a common analysis technique in electrical engineering which is used to approximate the behavior of nonlinear devices with linear equations. This linearization is formed about the DC bias point of the device (that is, the voltage/current levels present when no signal is applied), and can be accurate for small excursions about this point.

Due to the existence of a large number of power converters, the dynamic stability problem in distributed energy systems becomes increasingly important. Dynamic stability of power electronics systems has been studied for many years. The significance of knowing the system transient stability for an assortment of variations leads to the widespread use of small-signal modeling. Small-signal analysis and synthesis around certain operating points (steady state points) are often used to investigate both the interactions among several power electronic modules and the stability issues of the whole system.

3.2 Applications

It is a common analysis technique in electrical engineering, which is used to approximate the behavior of nonlinear devices through linear equations. It has been used for several decades in electronics [8-10] after the Lindholm-Hamilton theory [11] for systematic modeling of solid-state devices. It remains a very useful systematic method for power electronics [12-20].

Many electronic circuits, such as radio receivers, communications, and signal processing circuits, generally carry small time-varying (AC) signals on top of a constant (DC) bias. This suggests using a method akin to approximation by finite difference method to analyze relatively small perturbations about the bias point.

Any nonlinear device which can be described quantitatively using a formula can then be 'linearized' about a bias point by taking partial derivatives of the formula with respect to all governing variables. These partial derivatives can be associated with physical quantities (such as capacitance, resistance and inductance), and a circuit diagram relating them can be formulated. Small-signal models exist for electron tubes, diodes, field-effect transistors (FET) and bipolar transistors, notably the hybrid-pi model and various two-port networks.

AC Analysis; tweak around the bias condition, i.e. around the DC bias of the circuit, add a small AC source that slightly increases and decreases the bias point.

“Linearize” the device. Replace the non-linear device with linear ones. If you take the instantaneous slope of the IV curve at a particular DC point and zoom into it, for values very close to this DC point, the IV curve looks quite linear.

Construct the small-signal model using values for the parameters that you found in Step 3 of Large-Signal Analysis.

Use this model to find things like gain, input and output resistances

3.3 Power system dynamic performance

To describe power system dynamic performance, differential equations can be expressed as a set of n first order, nonlinear, ordinary differential equations. These can be represented in the state-variable form as the vector equations:

$$\dot{x} = f(x, u) \tag{3.1}$$

Where,

$$x = \begin{bmatrix} x_1 \\ x_2 \\ \vdots \\ x_n \end{bmatrix} \tag{3.2}$$

$$f = \begin{bmatrix} f_1 \\ f_2 \\ \vdots \\ f_n \end{bmatrix} \tag{3.3}$$

$$u = \begin{bmatrix} u_1 \\ u_2 \\ \vdots \\ u_n \end{bmatrix} \tag{3.4}$$

The column vector x is referred to as the state vector, x_i as the state variables. The column vector u is the vector of inputs to the system.

$$y = g(x, u) \tag{3.5}$$

Where,

$$y = \begin{bmatrix} y_1 \\ y_2 \\ \vdots \\ y_n \end{bmatrix} \tag{3.6}$$

$$g = \begin{bmatrix} g_1 \\ g_2 \\ \vdots \\ g_n \end{bmatrix} \tag{3.7}$$

The column vector y is the vector of inputs, and g is the vector of nonlinear functions relating state and input variables to output variables. The equilibrium point or singular point is the point whose trajectory speed is zero. From the mathematical view, it must satisfy the following equation:

$$f(x_0, u_0) = 0 \tag{3.8}$$

The stability of any hyperbolic equilibrium point x_0 of Eq. (3.1) is determined by the signs of the real parts of the eigenvalues of the matrix $Df(x_0)$.

A method, originated by Lyapunov, is very useful for determining the stability of non-hyperbolic equilibrium points.

Based on Lyapunov theory, if a small-signal linear model is valid near an equilibrium state and it is stable, then there is a region containing the equilibrium state in which the nonlinear system is stable. From this concept, the system model can be linearized within the neighborhood of the equilibrium point.

Here is an expansion of the nonlinear equation in terms of perturbations from these equilibrium values:

$$x = x_0 + \tilde{x} \tag{3.9}$$

$$u = u_0 + \tilde{u} \tag{3.10}$$

The nonlinear function can be expressed in terms of Taylor's series expansion. Neglecting the second and higher order powers, the equations become:

$$\dot{\tilde{x}} = A\tilde{x} + B\tilde{u} \tag{3.11}$$

$$\tilde{y} = C\tilde{x} + D\tilde{u} \tag{3.12}$$

Where $A=Df(x_0)$.

Then the equilibrium point x0 has been translated to the origin of the linear system.

We can use the eigenvalues to study the small-signal stability of the operating point. It is apparent that the system is locally stable if all of the eigenvalues are on the left-hand side of the imaginary axis of the complex plane. Otherwise, if at least one of the eigenvalues appears on the right of this axis, the corresponding modes are said to be unstable. This is confirmed by looking at the time dependent characteristic of the 19 oscillatory modes corresponding to each eigenvalue λ_i, given by $e^{\lambda i}$. The latter part shows that a real eigenvalue corresponds to a non-oscillatory mode. If the real part of the eigenvalue is negative, the mode decays over time. If the real part of the eigenvalue is positive, the mode is said to have aperiodic instability.

On the other hand, conjugate complex eigenvalues correspond to oscillatory modes. A pair with a positive real part represents an unstable oscillatory mode since eigenvalues yield an unstable time response of the system.

Therefore, small-signal modeling and analysis for parallel connected converters is used to explore the characteristics of their system, and to select system and controller parameters, and thus become indispensable and unavoidable tasks for system designers.

3.4 Small signal stability

Small signal stability in a power system is the ability of the system to ascertain a stable operating condition following a small perturbation around its operating equilibrium. Power

system disturbances can be broadly classified into two categories; large and small. Disturbances such as generation tripping, load outage, faults etc. have severe influences on the system operation. These are large disturbances and the dynamic response and the stability conditions of the system are assessed within the standard framework of transient stability analysis and control. The system is modeled as a non-linear dynamic process. A large number of references dealing with this problem exist in power engineering literature. Essentially the researchers have applied non-linear system theories and simulations to establish a clear understanding of the dynamic behavior of power system under such conditions. Effective tools to analyze and devise various non-linear control strategies are now in place.

In order to study the influence of system parameters on the stability and dynamic performance of combination-configuration PMSG based wind turbine, small-signal model is established at the point of steady state. By calculating the eigenvalues of state matrix, the small-signal stability of combination-configuration PMSG can be directly analyzed. Based on sensitivity analysis, the key parameters influencing on each eigenvalue are found out. Using root locus method, the ranges of key parameters and their influence on dynamic performance are determined. Analysis result shows the presented method provides the basis for the optimization design of key parameters, and is helpful to improve the stability and dynamics performance of islanding PMSG.

This model is used as a starting point in the development of a more comprehensive model. The accuracy of the new model is verified through comparisons of small-signal dynamic predictions, simulations, and experimental results.

For studying the stability of wind turbine with direct drive permanent magnet synchronous generator connected to power grid after suffering a small disturbance and effectively designing the controllers' parameters, a complete small signal model of the system is built. By means of eigenvalue analysis, the relation between the modes and state variables can be discovered. Then, the influences of the controllers' parameters on the traces of eigenvalues are analyzed, which helps to design controllers' parameters. A simulation model of the system based on MATLAB/SIMULINK is presented. The simulation results show that the system is stable after suffering small disturbance of a wind velocity step down and a step up, and the system dynamic responses are consistent with the result of small-signal analysis.

Traditional linear control techniques may be used to improve the performance and stability of the system. This is a demonstrated in an analysis of the system's eigenvalues. Drawing from the insights provided by this analysis, hardware and control parameters are selected to improve the response of the generic inverter.

The concept of Virtual Synchronous Machines (VSMs) is emerging as a flexible approach for controlling power electronic converters in grid-connected as well as in stand-alone applications. Several VSM implementations have been proposed, with the emulation of inertia and damping of a traditional Synchronous Machine (SM) as their common feature.

A virtual swing equation provides the phase orientation of cascaded voltage and current controllers in a synchronous reference frame. The control system also includes a virtual

impedance and an outer loop frequency droop controller which is functionally equivalent to the governor of a traditional SM.

The inherent capability of the investigated PMSG implementation to operate in both grid-connected and islanded mode is demonstrated by numerical simulations. Then, a linearized small-signal model of the PMSG operated while feeding a local load is developed and verified by comparing its dynamic response to the time-domain simulation of a nonlinear system model. Finally, this small-signal model is applied to identify the dominant modes of the system and to investigate their parametric sensitivity.

Chapter 4

Permanent magnet synchronous generator

4.1 Permanent magnet

Magnets that keeps their magnetic fields for a long periods in varying conditions are called permanent magnet. Permanent magnets are typically not made of iron, which can lose magnetic strength over time. A type of magnet called a rare-earth magnet can be formed into shapes needed to fit inside a PMSG.

A good permanent magnet should produce a high magnetic field with a low mass, and should be stable against the influences which would demagnetize it. The desirable properties of such magnets are typically stated in terms of the remanence and coercivity of the magnet materials. When a ferromagnetic material is magnetized in one direction, it will not relax back to zero magnetization when the imposed magnetizing field is removed. The amount of magnetization it retains at zero driving field is called its remanence. In this thesis book there is nothing. If you want to know about our work just call me. You have to find out who am I. We did a lot of things in this topic. It must be driven back to zero by a field in the opposite direction; the amount of reverse driving field required to demagnetize it is called its coercivity. If an alternating magnetic field is applied to the material, its magnetization will trace out a loop called a hysteresis loop. The lack of retrace ability of the magnetization curve is the property called hysteresis and it is related to the existence of magnetic domains in the material. Once the magnetic domains are reoriented, it takes some energy to turn them back again. This property of ferromagnetic materials is useful as a magnetic "memory". Some compositions of ferromagnetic materials will retain an imposed magnetization indefinitely and are useful as "permanent magnets".

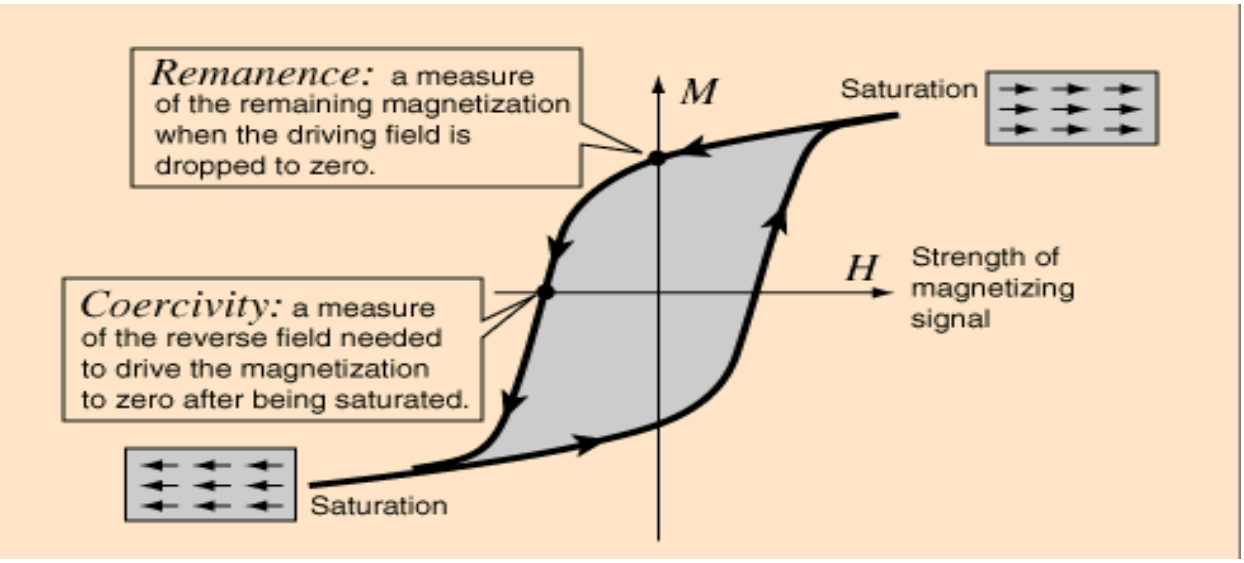

Fig 4.1: Hysteresis curve of a permanent magnet.

The table below contains some data about materials used as permanent magnets. Both the coercivity and remanence are quoted in Tesla, the basic unit for magnetic field B. The hysteresis loop above is plotted in the form of magnetization M as a function of driving magnetic field strength H. This practice is commonly followed because it shows the external driving influence (H) on the horizontal axis and the response of the material (M) on the vertical axis. Besides coercivity and remanence, a quality factor for permanent magnets is the quantity (BB0/μ0) max. A high value for this quantity implies that the required magnetic flux can be obtained with a smaller volume of the material, making the device lighter and more compact.

Table 4.1

Materials	Coercivity (T)	Remanence (T)	$(BB_0/\mu_0)_{max}$ (kJ/m^3)
$BaFe_{12}O_{19}$	0.36	0.36	25
Alnico IV	0.07	0.6	10.3
Alnico V	0.07	1.35	55
Alcomax I	0.05	1.2	27.8
MnBi	0.37	0.48	44
$Ce(CuCo)_5$	0.45	0.7	92
$SmCo_5$	1	0.83	160
Sm_2Co_{17}	0.6	1.15	215
$Nd_2Fe_{14}B$	1.2	1.2	260

Data from Myers [21]

The alloys from which permanent magnets are made are often very difficult to handle metallurgically. They are mechanically hard and brittle. They may be cast and then ground into shape, or even ground to a powder and formed. From powders, they may be mixed with resin binders and then compressed and heat treated. Maximum anisotropy of the material is desirable, so to that end the materials are often heat treated in the presence of a strong magnetic field.
The materials with high remanence and high coercivity from which permanent magnets are made are sometimes said to be "magnetically hard" to contrast them with the "magnetically soft" materials from which transformer cores and coils for electronics are made.

4.2 Rare Earth Magnets

The permanent magnets which have produced the largest magnetic flux with the smallest mass are the rare earth magnets based on samarium and neodymium. Their high magnetic fields and light weight make them useful for demonstrating magnetic levitation over superconducting materials.

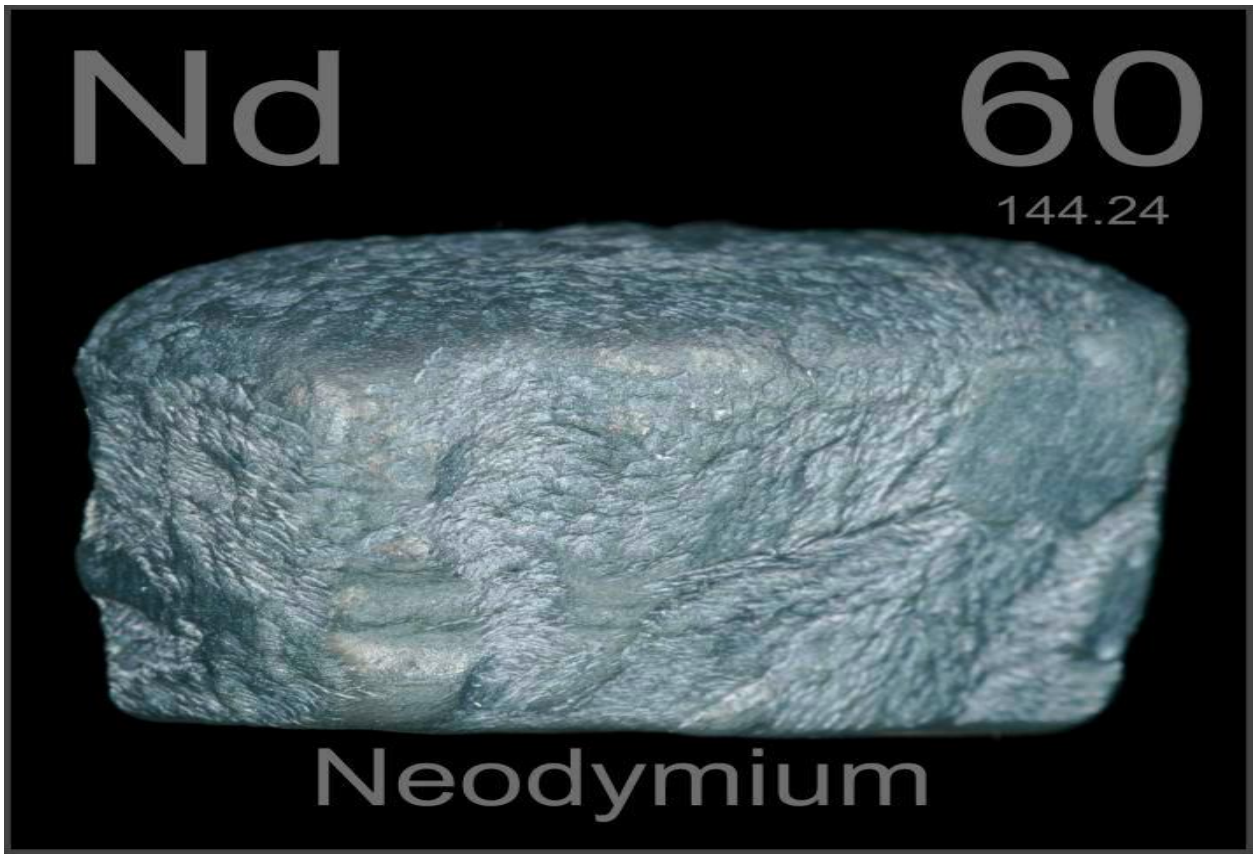

Fig 4.2: Neodymium.

The samarium-cobalt combinations have been around longer, and the $SmCo_5$ magnets are produced for applications where their strength and small size offset the disadvantage of their high cost. The more recent neodymium materials like $Nd_2Fe_{14}B$ produce comparable performance, and the raw alloy materials cost about 1/10 as much. They have begun to find application in microphones and other applications that exploit their high field and light weight. The production is still quite costly since the raw alloy must be ground to powder, pressed into the desired shape and then sintered to make a durable solid.

Table 4.2

Materials	Coercivity (T)	Remanence (T)	$(BB_0/\mu_0)_{max}$ (kJ/m^3)
$SmCo_5$	1	0.83	160
Sm_2Co_{17}	0.6	1.15	215
$Nd_2Fe_{14}B$	1.2	1.2	260

Data from Myers [21]

4.3 Types of permanent magnet used in PMSG

There are several types of permanent magnet used in PMSG. These are

- Alnico: Aluminum Nickel Cobalt
- Fe_3O_4: Ceramic/Ferrite
- $SmCo_5$: Samarium Cobalt
- NeFeBo: Neodymium Iron Boron

4.3.1 Alnico: Aluminum Nickel Cobalt

Alnico is an acronym[22] referring to a family of iron alloys which in addition to iron are composed primarily of aluminum (Al), nickel (Ni) and cobalt (Co), hence al-ni-co. They also include copper, and sometimes titanium. Alnico alloys are ferromagnetic, with a high coercivity (resistance to loss of magnetism) and are used to make permanent magnets. Before the development of rare earth magnets in the 1970s, they were the strongest type of magnet. Other trade names for alloys in this family are: Alni, Alcomax, Hycomax, Columax, and Ticonal. [23]

The composition of alnico alloys is typically 8–12% Al, 15–26% Ni, 5–24% Co, up to 6% Cu, up to 1% Ti, and the balance is Fe. The development of alnico began in 1931, when T. Mishima in Japan discovered that an alloy of iron, nickel, and aluminum had a coercivity of 400 oersted (Oe; 32 kA/m), double that of the best magnet steels of the time. [24]

Properties

Alnico alloys make strong permanent magnets, and can be magnetized to produce strong magnetic fields. Of the more commonly available magnets, only rare-earth magnets such as neodymium and samarium-cobalt are stronger. Alnico magnets produce magnetic field strength at their poles as high as 1500 gauss (0.15 tesla), or about 3000 times the strength of Earth's magnetic field. Some brands of alnico are isotropic and can be efficiently magnetized in any direction. Other types, such as alnico 5 and alnico 8, are anisotropic, with each having a preferred direction of magnetization, or orientation. Anisotropic alloys generally have greater magnetic capacity in a preferred orientation than isotropic types. Alnico's remanence (Br) may exceed 12,000 G (1.2 T) [clarification needed], its coercivity (Hc) can be up to 1000 oersted (80 kA/m), its energy product ((BH) max) can be up to 5.5 MG·Oe (44 T·A/m). This means alnico can produce a strong magnetic flux in closed magnetic circuit, but has relatively small resistance against demagnetization.

Alnico alloys have some of the highest Curie temperatures of any magnetic material, around 800 °C (1,470 °F), although the maximum working temperature is normally limited to around 538 °C (1,000 °F). [25] They are the only magnets that have useful magnetism even when heated red-hot. [26] This property, as well as its brittleness and high melting point, is the result of the strong tendency toward order due to intermetallic bonding between aluminum and its other constituents. They are also one of the most stable magnets if they are handled properly. Alnico magnets are electrically conductive, unlike ceramic magnets. As of 2008, Alnico magnets cost about $44/kg ($20/pound) or $4.30/BHmax. [30]

Table 4.3

Magnetic Materials	Density(g/cm)	Maximum Energy Product BH (max) (MGOe?)	Residual Induction Br	Coercive Force Hc	Intrinsic Coercive Force Hc	Normal Maximum Operating Temp F°
Alnico 5 (cast)	7.3	5.5	12800	640	640	975
Alnico 8 (cast)	7.3	5.3	8200	1650	1860	1020
Alnico 5 (sintered)	6.9	3.9	10900	620	630	975
Alnico 8 (sintered)	7.0	4.0	7400	1500	1690	1020

Reference [6]

Classification

Alnico magnets are traditionally classified using numbers assigned by the Magnetic Materials Producers Association (MMPA), for example, alnico 3 or alnico 5. These classifications indicate chemical composition and magnetic properties. (The classification numbers themselves do not have any direct relation to the properties of the magnet; for instance, a higher number does not necessarily indicate a stronger magnet.)[27]

These classification numbers, while still in use, have been deprecated in favor of a new system by the MMPA, which designates Alnico magnets based on maximum energy product in megagauss-oersteds and intrinsic coercive force as kilooersteds, as well as an IEC classification system. [27]

Manufacturing process

Alnico magnets are produced by casting or sintering processes. [28] Anisotropic alnico magnets are oriented by heating above a critical temperature, and cooling in the presence of a magnetic field. Both isotropic and anisotropic alnico require proper heat treatment to develop optimum magnetic properties — without it alnico's coercivity is about 10 Oe, comparable to technical iron, which is a soft magnetic material. After the heat treatment alnico becomes a composite material, named "precipitation material"—it consists of iron and cobalt rich [29] precipitates in rich-NiAl matrix.

Alnico's anisotropy is oriented along the desired magnetic axis by applying an external magnetic field to it during the precipitate particle nucleation, which occurs when cooling from

00 °C (1,650 °F) to 800 °C (1,470 °F), near the Curie point. Without an external field there are local anisotropies of different orientations, due to spontaneous magnetization. The precipitate structure is a "barrier" against magnetization changes, as it prefers few magnetization states requiring much energy to get the material into any intermediate state. Also, a weak magnetic field shifts the magnetization of the matrix phase only, and is reversible.

4.3.2 Fe_3O_4: Ceramic/Ferrite

A ferrite is a type of ceramic compound composed of iron oxide (Fe_2O_3) combined chemically with one or more additional metallic elements. [31] They are both electrically nonconductive and ferrimagnetic, meaning they can be magnetized or attracted to a magnet. Ferrites can be divided into two families based on their magnetic coercivity, their resistance to being demagnetized. Hard ferrites have high coercivity; they are difficult to demagnetize. They are used to make magnets, for devices such as refrigerator magnets, loudspeakers and small electric motors. Soft ferrites have low coercivity. They are used in the electronics industry to make ferrite cores for inductors and transformers, and in various microwave components. Yogoro Kato and Takeshi Takei of the Tokyo Institute of Technology invented ferrite in 1930. [32]

Composition and properties

Ferrites are usually non-conductive ferrimagnetic ceramic compounds derived from iron oxides such as hematite (Fe_2O_3) or magnetite (Fe_3O_4) as well as oxides of other metals. Ferrites are, like most of the other ceramics, hard and brittle.

Many ferrites are spinels with the formula AB_2O_4, where A and B represent various metal cations, usually including iron Fe. Spinel ferrites usually adopt a crystal motif consisting of cubic close-packed (fcc) oxides (O^{2-}) with A cations occupying one eighth of the tetrahedral holes and B cations occupying half of the octahedral holes. If one eighth of the tetrahedral holes are occupied by B cation, then one fourth of the octahedral sites are occupied by A cation and the other one fourth by B cation and it's called the inverse spinel structure. It's also possible to have mixed structure spinel ferrites with formula $[M^{2+}_{1-\delta}Fe^{3+}_{\delta}]\ [M^{2+}_{\delta}Fe^{3+}_{2-\delta}]O_4$ where δ is the degree of inversion.

The magnetic material known as "ZnFe" has the formula $ZnFe_2O_4$, with Fe^{3+} occupying the octahedral sites and Zn^{2+} occupy the tetrahedral sites, and it’s an example of normal structure spinel ferrite. [33]

Some ferrites have hexagonal crystal structure, like Barium and Strontium ferrites $BaFe_{12}O_{19}$ (BaO: 6Fe2O3) and $SrFe_{12}O_{19}$ (SrO: 6Fe2O3). [34]

In terms of their magnetic properties, the different ferrites are often classified as "soft" or "hard", which refers to their low or high magnetic coercivity, as follows.

Soft ferrites

Various ferrite cores used to make small transformers and inductors

Ferrites that are used in transformer or electromagnetic cores contain nickel, zinc, and/or manganese compounds. They have a low coercivity and are called **soft** ferrites. The low

coercivity means the material's magnetization can easily reverse direction without dissipating much energy (hysteresis losses), while the material's high resistivity prevents eddy currents in the core, another source of energy loss. Because of their comparatively low losses at high frequencies, they are extensively used in the cores of RF transformers and inductors in applications such as switched and loop stick antennas used in AM radios.

The most common soft ferrites are:

- **Manganese-zinc ferrite** (MnZn, with the formula $Mn_aZn_{(1-a)}Fe_2O_4$). MnZn have higher permeability and saturation induction than NiZn.
- **Nickel-zinc ferrite** (NiZn, with the formula $Ni_aZn_{(1-a)}Fe_2O_4$). NiZn ferrites exhibit higher resistivity than MnZn, and are therefore more suitable for frequencies above 1 MHz.

For applications below 5 MHz, MnZn ferrites are used; above that, NiZn is the usual choice. The exception is with common mode inductors, where the threshold of choice is at 70 MHz.

Hard ferrites

In contrast, permanent ferrite magnets are made of **hard ferrites**, which have a high coercivity and high remanence after magnetization. Iron oxide and barium or strontium carbonate are used in manufacturing of hard ferrite magnets. [36] The high coercivity means the materials are very resistant to becoming demagnetized, an essential characteristic for a permanent magnet. They also have high magnetic permeability. These so-called *ceramic magnets* are cheap, and are widely used in household products such as refrigerator magnets. The maximum magnetic field *B* is about 0.35 tesla and the magnetic field strength *H* is about 30 to 160 kilo ampere turns per meter (400 to 2000oersteds). [37] The density of ferrite magnets is about 5 g/cm^3.

The most common hard ferrites are:

- **Strontium ferrite**, $SrFe_{12}O_{19}$ ($SrO{\cdot}6Fe_2O_3$), used in small electric motors, micro-wave devices, recording media, magneto-optic media, telecommunication and electronic industry. [34]
- **Barium ferrite**, $BaFe_{12}O_{19}$ ($BaO{\cdot}6Fe_2O_3$), a common material for permanent magnet applications. Barium ferrites are robust ceramics that are generally stable to moisture and corrosion-resistant. They are used in e.g. loudspeaker magnets and as a medium for magnetic recording, e.g. on magnetic stripe cards.
- **Cobalt ferrite**, $CoFe_2O_4$ ($CoO{\cdot}Fe_2O_3$), used in some media for magnetic recording.

Production

Ferrites are produced by heating a mixture of finely-powdered precursors pressed into a mold. During the heating process, calcination of carbonates occurs:

$$MCO_3 \rightarrow MO + CO_2$$

The oxides of barium and strontium are typically supplied as their carbonates, $BaCO_3$ or $SrCO_3$. The resulting mixture of oxides undergoes sintering. Sintering is a high temperature process similar to the firing of ceramic ware.

Afterwards, the cooled product is milled to particles smaller than 2 µm, small enough that each particle consists of a single magnetic domain. Next the powder is pressed into a shape, dried, and re-sintered. The shaping may be performed in an external magnetic field, in order to achieve a preferred orientation of the particles (anisotropy).

Small and geometrically easy shapes may be produced with dry pressing. However, in such a process small particles may agglomerate and lead to poorer magnetic properties compared to the wet pressing process. Direct calcination and sintering without re-milling is possible as well but leads to poor magnetic properties.

Electromagnets are pre-sintered as well (pre-reaction), milled and pressed. However, the sintering takes place in a specific atmosphere, for instance one with an oxygen shortage. The chemical composition and especially the structure vary strongly between the precursor and the sintered product.

To allow efficient stacking of product in the furnace during sintering and prevent parts sticking together, many manufacturers separate ware using ceramic powder separator sheets. These sheets are available in various materials such as alumina, zirconia and magnesia. They are also available in fine, medium and coarse particle sizes. By matching the material and particle size to the ware being sintered, surface damage and contamination can be reduced while maximizing furnace loading.

4.3.3 $SmCo_5$: Samarium Cobalt

A samarium–cobalt (SmCo) magnet, a type of rare earth magnet, is a strong permanent magnet made of an alloy of samarium and cobalt. They were developed in the early 1970s by Albert Gale and Dilip K. Das of Raytheon Corporation. [38] They are generally ranked similarly in strength to neodymium magnets, but have higher temperature ratings and higher coercivity. They are brittle, and prone to cracking and chipping. Samarium–cobalt magnets have maximum energy products (BH_{max}) that range from 16 megagauss-oersteds (MGOe) to 33 MGOe, that is approx. 128 kJ/m^3 to 264 kJ/m^3; their theoretical limit is 34 MGOe, about 272 kJ/m^3. They are available in two "series", namely Series 1:5 and Series 2:17.

Sintered Samarium Cobalt magnets exhibit magnetic anisotropy, meaning they can only be magnetized in the axis of their magnetic orientation. This is done by aligning the crystal structure of the material during the manufacturing process.

These samarium–cobalt magnet alloys (generally written as $SmCo_5$, or SmCo Series 1:5) have one atom of rare earth samarium and five atoms of cobalt. By weight this magnet alloy will typically contain 36% samarium with the balance cobalt. The energy products of these samarium–cobalt alloys range from 16 MGOe to 25 MGOe, what is approx. 128 kJ/m^3 - 200 kJ/m^3. These samarium–cobalt magnets generally have a reversible temperature coefficient of -0.05%/°C. Saturation magnetization can be achieved with a moderate magnetizing field. This

series of magnet is easier to calibrate to a specific magnetic field than the SmCo 2:17 series magnets.

In the presence of a moderately strong magnetic field, unmagnetized magnets of this series will try to align their orientation axis to the magnetic field, thus becoming slightly magnetized. This can be an issue if postprocessing requires that the magnet be plated or coated. The slight field that the magnet picks up can attract debris during the plating or coating process, causing coating failure or a mechanically out-of-tolerance condition. Samarium - cobalt magnet has a strong resistance to corrosion and oxidation resistance, usually do not need to be coated can be widely used in high temperature and poor working conditions. [39]

Reversible temperature coefficient

B_r drifts with temperature and it is one of the important characteristics of magnet performance. Some applications, such as inertial gyroscopes and travelling wave tubes (TWTs), need to have constant field over a wide temperature range. The reversible temperature coefficient (RTC) of B_r is defined as

$$(\Delta B_r/B_r) \text{ x } (1/\Delta \text{ T}) \times 100\%.$$

To address these requirements, temperature compensated magnets were developed in the late 1970s. For conventional SmCo magnets, B_r decreases as temperature increases. Conversely, for GdCo magnets, B_r increases as temperature increases within certain temperature ranges. By combining samarium and gadolinium in the alloy, the temperature coefficient can be reduced to nearly zero.

Coercivity mechanism

$SmCo_5$ magnets have a very high coercivity (coercive force); that is, they are not easily demagnetized. They are fabricated by packing wide-grain lone-domain magnetic powders. All of the magnetic domains are aligned with the easy axis direction. In this case, all of the domain walls are at 180 degrees. When there are no impurities, the reversal process of the bulk magnet is equivalent to lone-domain motes, where coherent rotation is the dominant mechanism. However, due to the imperfection of fabricating, impurities may be introduced in the magnets, which form nuclei. In this case, because the impurities may have lower anisotropy or misaligned easy axes, their directions of magnetization are easier to spin, which breaks the 180° domain wall configuration. In such materials, the coercivity is controlled by nucleation. To obtain much coercivity, impurity control is critical in the fabrication process.

Machining samarium–cobalt

The alloys are typically machined in the unmagnetized state. Samarium–cobalt should be ground using a wet grinding process (water based coolants) and a diamond grinding wheel. The same type of process is required if drilling holes or other features that are confined. The grinding waste produced must not be allowed to completely dry as samarium–cobalt has a low ignition point. A small spark, such as that produced with static electricity, can easily commence combustion. The fire produced will be extremely hot and difficult to control.

Production

The reduction/melt method and reduction/diffusion method are used to manufacture samarium–cobalt magnets. The reduction/melt method will be described since it is used for both $SmCo_5$ and Sm_2Co_{17} production. The raw materials are melted in an induction furnace filled with argon gas. The mixture is cast into a mold and cooled with water to form an ingot. The ingot is pulverized and the particles are further milled to further reduce the particle size. The resulting powder is pressed in a die of desired shape, in a magnetic field to orient the magnetic field of the particles. Sintering is applied at a temperature of 1100˚C–1250˚C, followed by solution treatment at 1100˚C–1200˚C and tempering is finally performed on the magnet at about 700˚C–900˚C. It then is ground and further magnetized to increase its magnetic properties. The finished product is tested, inspected and packed.

Hazards

- Samarium–cobalt magnets can easily chip; eye protection must be worn when handling them.
- Allowing magnets to snap together can cause the magnets to shatter, which can cause a potential hazard.
- Samarium–cobalt is manufactured by a process called sintering, and as with all sintered materials, inherent cracks are very possible. These magnets do not have mechanical integrity; instead the magnet must be utilized for its magnetic functions and other mechanical systems must be designed to provide the mechanical reliability of the system.

Attributes

- Extremely resistant to demagnetization
- Good temperature stability (maximum use temperatures between 250 °C (523 K) and 550 °C (823 K); Curie temperatures from 700 °C (973 K) to 800 °C (1,070 K)
- Expensive and subject to price fluctuations (cobalt is market price sensitive)

4.3.4 NeFeBo: Neodymium Iron Boron

Sintered neodymium-iron-boron (NdFeB) magnets, also referred to as "neo" magnets, have been commercially available since November 1984. They offer the highest energy product of any material today and are available in a very wide range of shapes, sizes and grades. Earliest use of neo magnets was primarily for voice coil motors (VCM's) in hard disk drives and this market still accounts for about 55% of total sales dollars. Other applications include high performance motors, brushless DC motors, magnetic separation, magnetic resonance imaging, sensors and loudspeakers.

Maximum use temperature and corrosion

The first materials produced achieved about half the theoretical maximum energy product of 64 MGOe (509 kJ/m3). Refinements over the past few years have allowed commercial supply of magnets close to 50 MGOe (398 kJ/m3). High temperature (>180°C) compositions have been developed with intrinsic coercivity greater than 25,000 oersteds (1990 kA/m). Higher temperature materials, however, tend to have lower maximum energy products.

Although the Curie temperature for NdFeB materials is 310 degrees for 0% cobalt-containing material to greater than 370 degrees for 5% cobalt-containing, some irreversible loss of output may be expected at even moderate temperatures. Neo magnets also have a moderately high Reversible Temperature Coefficient of Induction which reduces total magnetic output as temperature rises. Selection of neo magnets instead of SmCo, for example, is a function of the maximum temperature of the application, required magnetic output at typical use temperature and total cost of the system.

Neo magnets also have some limitations due to their corrosion behavior. In humid applications, a protective coating is highly recommended. Coatings which have been used successfully include, E-coat (a liquid dip epoxy coating), dry electrostatic spray epoxy, nickel plating and combinations of these coatings. Changes in composition and processing over the past several years have resulted in significant improvements in corrosion resistance and high temperature performance.

Most of the rare earth elements (neodymium, dysprosium, samarium, etc.) absorb hydrogen into the structure resulting in expansion and cracking of the material which is referred to as decrepitating. Therefore, neo magnets are not recommended where exposure to hydrogen is likely.

Manufacturing

Neo magnets are typically produced via a powder metallurgy process wherein the alloy composition is melted from raw materials, crushed into a coarse powder, finely milled, compaction pressed, sintered and finish processed.

Arnold can provide both fully dense AND polymer or epoxy resin bonded neo magnets. For information on bonded neo, please visit the Bonded Magnet section.

Table 4.3

Comparison of physical properties of sintered neodymium and Sm-Co magnets [36]

Property	Neodymium	Sm-Co
Remanence (T)	1–1.3	0.82–1.16
Coercivity (MA/m)	0.875–1.99	0.493–1.59
Relative permeability	1.05	1.05

Temperature coefficient of remanence (%/K)	−0.12	−0.03
Temperature coefficient of coercivity (%/K)	−0.55..–0.65	−0.15..–0.30
Curie temperature (°C)	320	800
Density (g/cm^3)	7.3–7.5	8.2–8.4
CTE, magnetizing direction (1/K)	5.2×10^{-6}	5.2×10^{-6}
CTE, normal to magnetizing direction (1/K)	-0.8×10^{-6}	11×10^{-6}
Flexural strength (N/mm^2)	250	150
Compressive strength (N/mm^2)	1100	800
Tensile strength (N/mm^2)	75	35
Vickers hardness (HV)	550–650	500–650
Electrical resistivity (Ω·cm)	$(110–170)\times10^{-6}$	86×10^{-6}

Table 4.4

Magnetic material	Price $ per lb.	B_r max (gauss)	Coercivity (oersted)	Typical P	Curie Temp (^{0}C)	β(1/^{0}C)
Alnico (5-7)	40	12500	650	50-75	850	0.0001
Ferrite	7	4000	3600	10-20	450	0.002
NdFeB	100	11000	10000	2-5	320	0.001
SmCo	180	8000	7500	4-8	800	0.00045

[32]

4.4 PMSG

A generator where the excitation field is provided by a permanent magnet instead of a coil is permanent magnet synchronous generator (PMSG).

A direct drive wind energy systems cannot employ a conventional high speed (and low torque) electrical machines. Hartkopf et al. in [40] has shown that the weight and size of electrical machines increases when the torque rating increases for the same active power. Therefore, it is essential task of the machine designer to consider an electrical machine with high torque density, in order to minimize the weight and the size. In and it has been shown that PM synchronous machines have higher torque density compared with induction and

switched reluctance machines. Thus a PMSG is chosen for further studies in this work. However, since the cost effectiveness of PMSG is an important issue, low manufacturing cost has to be considered as a design criterion in further steps. There are a number of different PMSG topologies; some of them are very attractive from the technical point of view. However, some of the state of the art topologies suffer from complication in manufacturing process which results in high production costs. PM excitation offers many different solutions. The shape, the size, the position, and the orientation of the magnetization direction can be arranged in many different ways. Here, presented topologies include those of which are investigated for low speed applications or variable speed applications. This list encompasses radial or axial flux machines, longitudinal or transversal flux machines, inner rotor or outer rotor machines and interior magnet or exterior magnet machines. Slot less machines are not presented here.

As the construction basis PM synchronous machine describe as follow:

i. Stator

ii. Rotor

There are some different types of rotors. These are:

a. Axial and radial flux rotor

b. Longitudinal or Transversal rotor

c. Inner Rotor or Outer Rotor

4.5 Rotor mechanism

Air gap orientation can be identified in two different ways. Here a hypothetical normal vector to the air gap is adopted along the flux direction. The axis of the machines is assumed to be along the length of the machine in the cylindrical coordinate system. Relation of the normal vector with the axis of the machine decides the radial or axial topology. If the normal vector is perpendicular to axis, machine is called radial. If the normal vector is parallel with the axis, the machine is called axial.

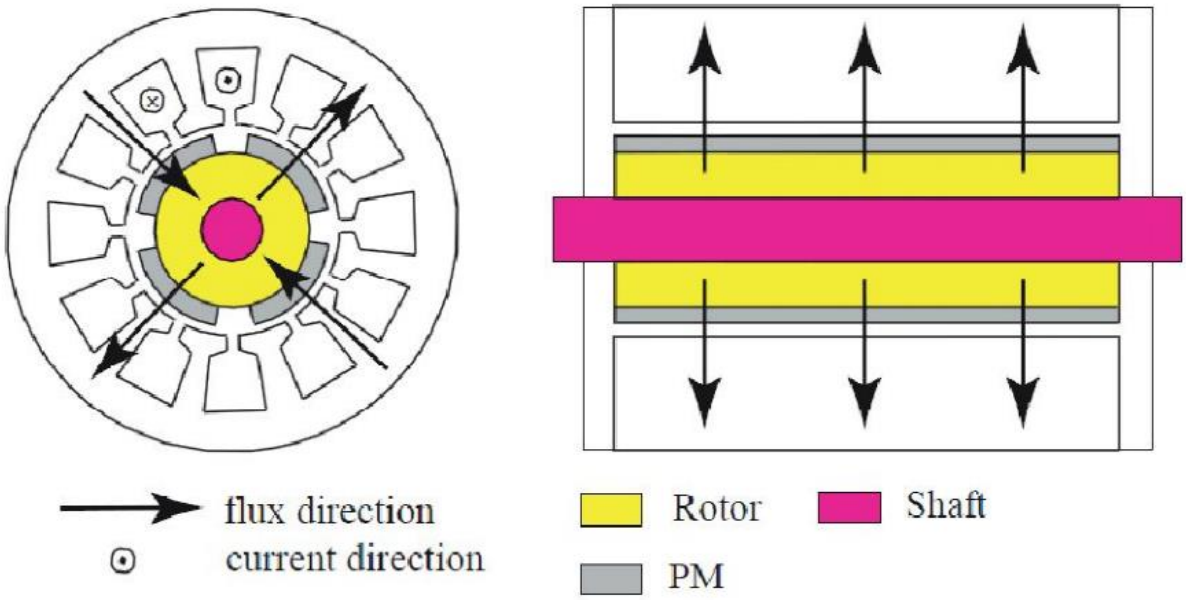

Fig 4.2: Cross sectional view in radial direction and in axial direction, respectively, of a typical radial flux PMSG [41].

Radial Flux Machines

Radial flux machines are conventional type of PMSG. The manufacturing technology is well established which makes the production cost lower compared with the axial one [2]. Furthermore, they are very flexible for scaling, as the higher power ratings of the machine are achieved by increasing the length of the machine. In other words completely new design and completely new geometry can be avoided. They are extensively used in ship propulsion, robotics, traction and wind systems. Figure 4.2 shows cross sectional view in radial direction and in axial direction, respectively, of a typical radial flux PMSG.

Axial Flux Machines

Various axial flux topologies have been proposed in recent years and their pros and cons are categorized. Generally, in axial flux machines length of the machine is much smaller compared with radial flux machines. Their main advantage is high torque density, so they are recommended for applications with size constraints especially in axial direction. They have found application in gearless elevator systems, and they are rarely used in traction, servo application, micro generation and propulsion systems [41]. Figure 4.3 shows cross sectional view in radial direction and in axial direction, respectively, of a typical axial flux PMSG . One of the disadvantages with the axial flux machines is that they are not balanced in single rotor single stator edition. Usually, for a better performance the rotor is sandwiched between two stators or vice versa.

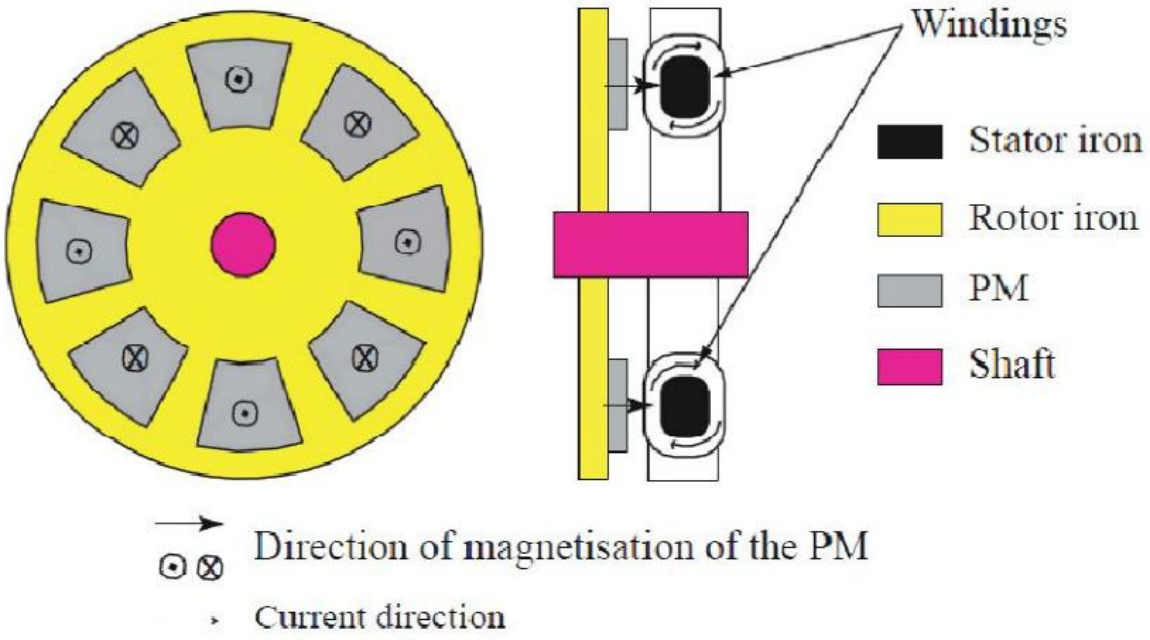

Fig 4.3: Cross sectional view in radial direction and in axial direction, respectively, of a typical axial flux PMSG [41].

Unlike radial flux machines, the stator windings are located in the radial direction. A circumferentially laminated stator is required for reduction of iron losses, which complicates manufacturing process. Scaling of axial flux machine is another drawback. Unlike radial flux machines, any increase in length is accompanied by increase in air gap diameter. Hence, to increase the power rating a new design and a new geometry is needed. One other way to increase the power rating is by increasing number of stators and rotors. This, however, makes the machine costly.

Longitudinal or Transversal

In transversal flux machines, the plane of flux path is perpendicular to the direction of rotor motion. The use of transversal flux machines can be proposed in applications with high torque density requirement. One attractive property of the transversal flux machines is that the current loading and the magnetic loading can be adjusted independently. They are proposed for wind systems, free piston generators for hybrid vehicles and ship propulsion [41]. Figure 4.4 shows a fraction of a typical transversal flux PMSG. Both PMSGs in Figures 4.4 and 4.5 are of longitudinal type.

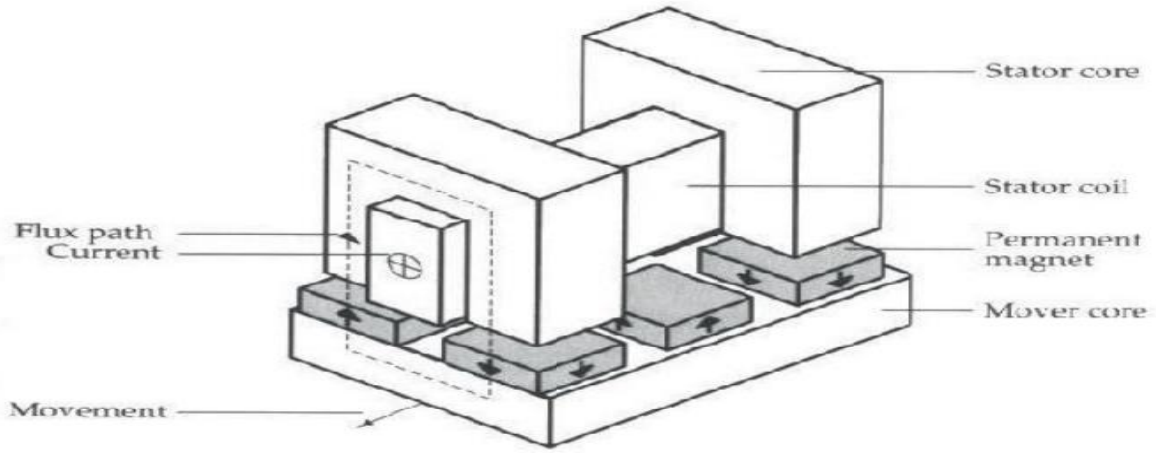

Fig 4.4: Fraction of a typical transversal flux PMSG [42].

One drawback of transverse PMSG is high leakage flux which results in poor power factor. To achieve lower flux leakage, number of poles has to be decreased which in turn reduces torque density. The task of the designer is to find a compromise between the flux leakage and the torque density of the machine. Further-more the major drawback with rotational ones is relatively difficult manufacturing process. Yet another drawback is that, in rotating transverse PMSG, mechanical construction is weak due to large number of parts.

Inner Rotor or Outer Rotor

The rotor surrounds the stator in outer rotor machines. In these machines, the magnets are usually located on the inner circumference of the rotor. Accordingly, for the same outer diameter of the machine, in the outer rotor machine the rotor has higher radius compared with the stator and it can be equipped with higher number of poles for the same pole pitch [41]. Another advantage is that the magnets are well supported despite the centrifugal force. Furthermore a better cooling of magnets is provided. Outer rotor machines are common for small HAWT turbines, where sometimes the hub carrying the blades is directly fixed to the rotor [41].

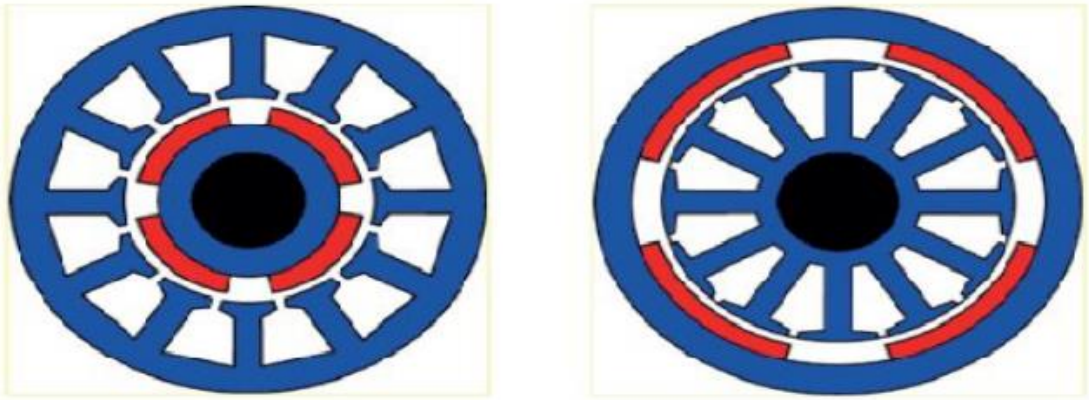

Fig 4.5: Inner rotor PMSG (left) and an outer rotor PMSG (right) [43].

However, the inner rotor machines are a more common solution present on the market today. In small machines, the main contributions to the losses are copper losses and therefore the stator winding has the highest temperature rise in the active material of the machine. Hence, it is more beneficial to put the stator winding, rather than the magnets, closer to the housing, where the cooling properties are good. This causes less temperature rise for the same amount of losses. Figure 4.5 shows an inner rotor PMSG and an outer rotor PMSG.

4.6 PM Configuration

The PMSG can be divided into different topologies depending on the magnet arrangement on the rotor. These are introduced below. However, it should be mentioned that the rotor configurations are not restricted to the given examples, e.g. In interior magnets various configurations are implementable.

Surface Mounted Magnets

A common topology is where the magnets are mounted on the surface of the rotor, sometimes referred to as exterior magnet, but, more known as Surface Mounted Permanent Magnet (SMPM) machine. The magnets are glued and/or bandaged to the rotor surface in order to withstand the centrifugal force. Usually, the magnets are oriented or magnetized in radial direction and more seldom in circumferential direction. The direct and quadrature reactances are almost equal. Construction of the rotor core in SMPM is the easiest among different PM configurations due to simple rotor geometry. Figure 4.6 shows a surface mounted rotor for a PMSG.

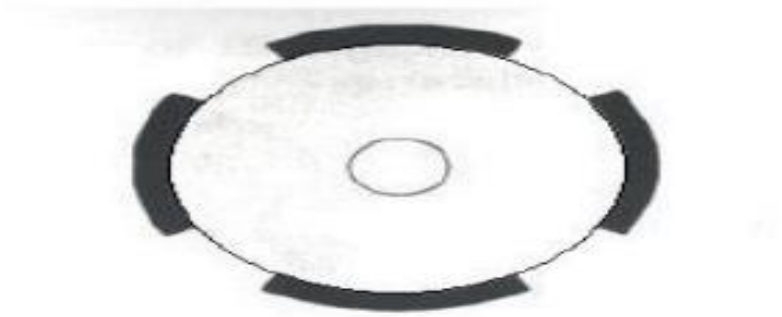

Fig: 4.6: A surface mounted rotor for a PMSG [44].

Inset Magnets

In inset magnet machines, rotor core of SMPM machine is modified with iron inter poles. Iron inter poles are protrusions of rotor core wherever magnets are not present on the surface. Inter poles cause saliency and the inductances in direct and quadrature directions are different. In these machines, part of the torque is reluctance torque and the torque density is higher compared to SMPM. The magnets are radially magnetized. The flux leakage is higher in comparison to SMPM which results in lower power factor. Therefore, in direct drive application, the inverter utilization is lower compared to geared applications. This topology is not common in gearless wind systems.

Buried Magnets

In this configuration the magnets are put inside the rotor and therefore it is referred to as Interior Permanent Magnet (IPM) machine. There are many different ways in achieving interior magnet configuration. The magnets can be magnetized in radial direction as well as circumferential direction. The thickness of iron bridges between the magnets has to be designed carefully to avoid saturation. Again, the inductance in quadrature axes is different from that in direct axes direction.

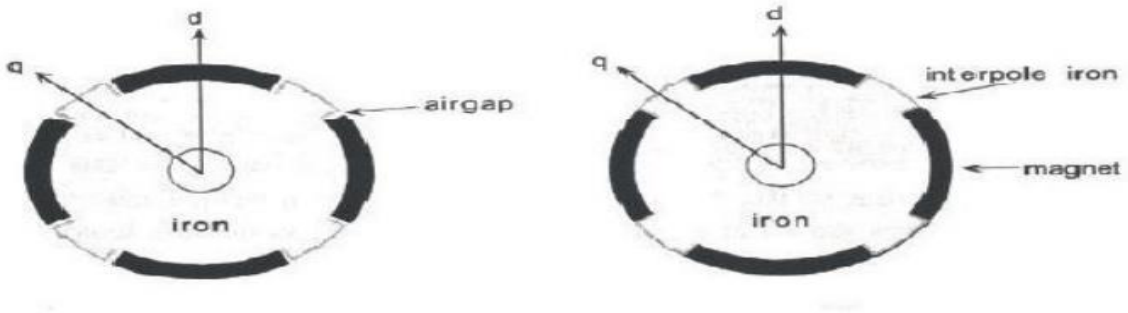

Fig 4.7: Two different inset magnet rotors for PMSGs [44].

The main advantage of this PM configuration is that weak PM material such as ferrite can be used. Another advantage is magnetic protection against short circuit conditions [44]. It is because in faulty conditions, iron bridges between magnets get saturated which prevents high reverse demagnetizing field to reach the magnets. This topology is suggested for high speed applications due to mechanical strength of the rotor against the centrifugal force. Burying magnets in production stage is a complicated process. Moreover a nonferromagnetic shaft is vital, otherwise a large part of magnets' flux penetrates the shaft, which is located nearby, and it will not be utilized for magnetization of the air gap. Like inset magnet machines, the flux leakage is high which reduces the power factor, the efficiency and the inverter utilization.

In [45], F. Libert studies two different buried magnet topologies and concludes that both gives rise to manufacturing problems. One is called V-shaped buried magnet design and the other is called tangentially magnetized buried magnet design. The author also mentions saturation problems when the number of poles is high. This is a common problem for the buried magnet topologies. If the number of poles increases, the distance between magnets decreases (when rotor core diameter is kept constant). Therefore, the narrow iron bridges get saturated more easily.

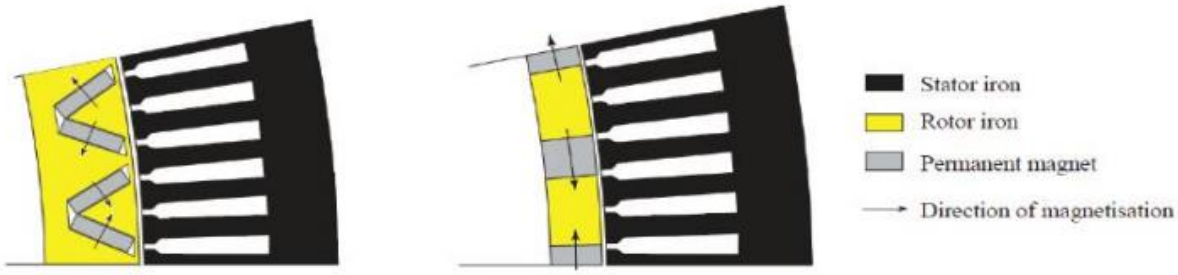

Fig 4.8: Cross section of a pole pair of a V shaped buried magnet design (left) and a tangentially buried magnet design (right) [45].

4.7 Windings

The windings can be divided into overlapping and non-overlapping categories. Over lapping windings can be wound either distributed or concentrated. Non overlapping windings can be wound solely in concentrated way. Figure 4.9.a) shows a distributed overlapping winding with Qs = 24 and q = 2 for a four pole machine. Figure 4.9.b) shows a concentrated overlapping winding with Qs = 12 and q = 1. Figure 4.9.c) shows a double layer concentrated non-overlapping winding with Qs = 6 and q = 0.5, which is the traditional concentrated winding. Figure 4.9.d) 30 shows a single layer concentrated non-overlapping winding with the same values of Qs and q). The term overlapping is usually omitted. For instance "overlapping distributed winding" is almost always referred to as distributed winding. In this text, on the other hand, "concentrated winding" stands for "double layer concentrated non -overlapping winding".

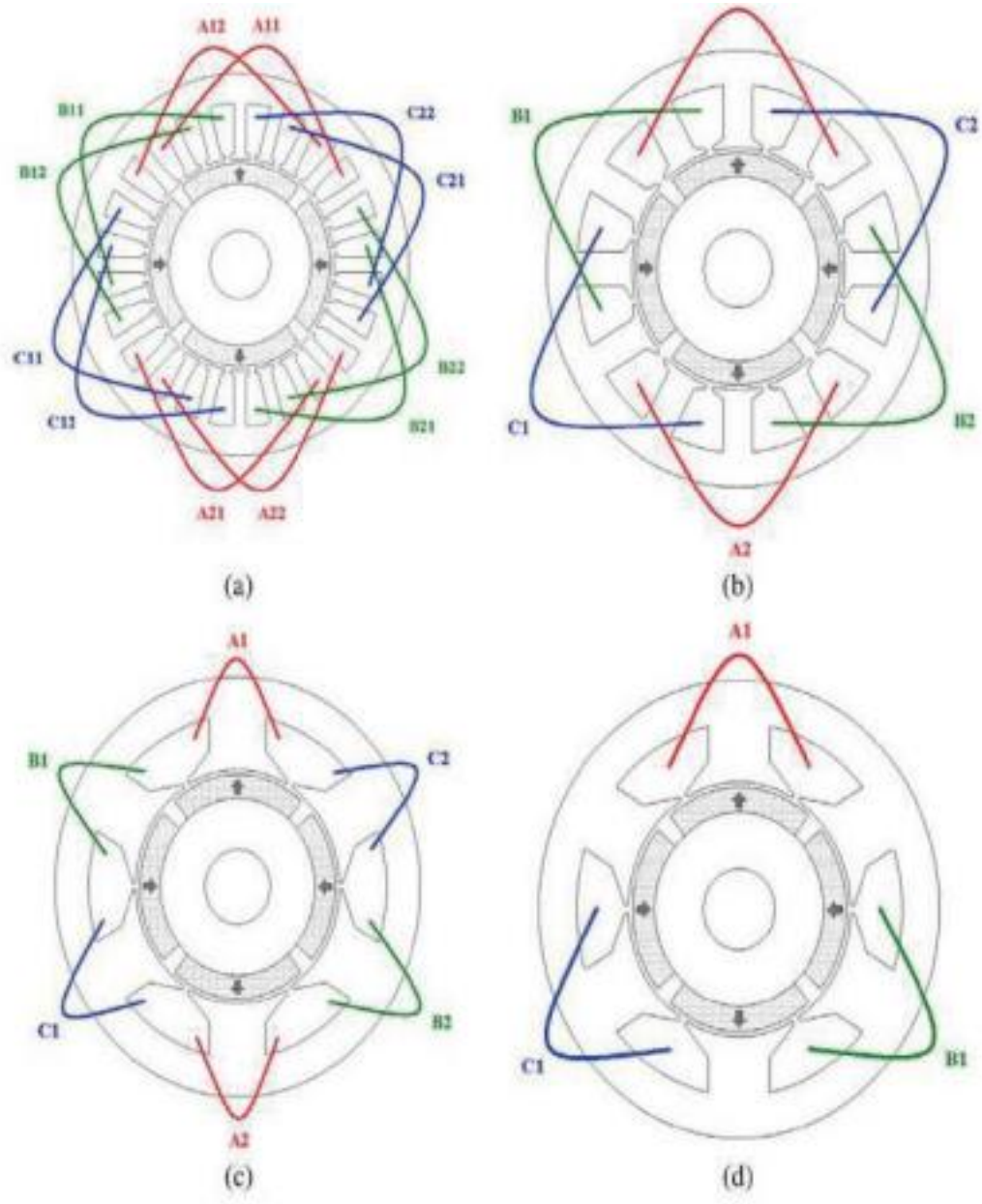

Fig 4.9: Windings in low speed PMSG a) distributed overlapping winding.

b) Concentrated overlapping winding. c) Double layer concentrated non-overlapping

Winding. d) Single layer concentrated non-overlapping winding [46].

Distributed Winding

Distributed winding has been used for Brushless Alternative Current (BLAC)machines for decades. One of the advantages of distributed winding is that it can give high value of winding factor when q is high and the full pole pitch is chosen. Nonetheless, it has some drawbacks, like for instance its long end windings. End windings do not contribute to induction

of the phase voltage. The role of end windings is limited to carry the current from one coil to the other. Thus, end windings are associated with copper losses and it is desired that the end windings are as short as possible. In distributed winding, when the coil sides are far from each other, the copper losses will be higher and the axial length of the machine will be longer. Thus distributed winding reduces the efficiency of the machine. If the size of the machine is a critical design parameter, the concentrated winding should be considered.

Concentrated Winding

In concentrated winding the coil turns are concentrated around one tooth and therefore it will benefit from short end windings due to non -overlapping property. Another advantage is better heat conductivity between the winding and the tooth. Furthermore, segmentation of stator core teeth is possible [47]. In this way, the windings can be pre-pressed and the coils can be made with rectangular shape, which, in turn, will give high slot fill factor and high torque density. Concentrated winding exhibits high fault tolerance on SMPM s and is associated with increase in leakage inductance [48]. Implementation of concentrated winding increases leakage inductance which in turn limits high currents in short circuit conditions. In fact in faulty conditions, the excitation field of WRSG is reduced to protect the machine. However, excitation of PMSG is not controllable. Hence, introduction of higher flux leakage may be an advantage. In addition, due to nonoverlapping property, coils are physically and thermally separated in a better way compared with distributed windings. This reduces the risk of phase to phase short circuit in the event of damaged winding insulation. Furthermore, the torque ripple in SMPMs with high pole numbers and concentrated windings is reduced [45]. Higher flux weakening capability is another characteristics of concentrated winding.

Fractional Slot Winding

One disadvantage with traditional concentrated winding, where q = 0.5, is a lower winding factor compared with distributed winding. The reason is that the slot pitch is 2/3 of the pole pitch and, neglecting the flux leakage due to iron saturation, only 2/3 of the magnet flux is linked to the stator. As a consequence, winding factor drops to 0.866 and torque rating of traditional concentrated winding is reduced by the same factor.

To cope with this drawback, fractional slot concentrated winding are suggested, which utilizes any feasible combination of p and Qs. Thus, it is possible to have higher winding factors with higher torque density. In applications where weight and size are critical design parameters, the fractional winding may be of interest. F. Magnussen in [16] and F. Libert in [15] have studied numerous slot pole number combinations of fractional slot winding and have categorized them regarding their parasitic effects. It has been reported that selection of pole and slot numbers has to be chosen very carefully because of the parasitic effects that arises with certain combinations. These parasitic effects include, cogging torque, radial magnetic forces and alternating magnetic fields with high frequency. The disadvantage with radial forces is vulnerability to magnetic noise, while high frequency magnetic flux leads to eddy current losses in the rotor and the magnets. Some counter active measures havebeen suggested by F. Magnussen like: magnet segmentation, rotor core lamination and high mechanical rigidity of core [15] 3. In [15] F. Libert has studied fractional slot winding in

terms of winding factor, harmonic content of Magneto-Motive Force (MMF) , torque ripple, cogging torque and magnetic forces. The study have been carried out on the design with pole numbers between 4 and 80 and slot numbers between 6 and 90. Slot pole number combinations are divided in few categories and general conclusions are drawn for each category. The categories where Least Common Multiple (LCM) is high, enjoys from the biggest reduction in cogging torque. The highest LCM is achieved where slot pole numbers have values very close to each other, i.e. $p = Qs \pm 1$. However, the machines with these combinations are asymmetrical. This gives rise to radial forces and magnetic noise. The 23 author, ultimately, suggests that the slot-pole number combinations with high winding factors and with symmetrical winding layouts have to be chosen. IPM s with concentrated winding have lower torque density than that with distributed winding. Concentrated winding decreases saliency ratio in IPM and accordingly the reluctance torque reduces as well. This means that an IPM with concentrated winding will have lower peak torque and also lower torque density. Reduction of torque density can be compensated with additional iron laminations in axial direction as the length of the machine become shorter due to concentrated windings; This, however, is costly

Single Layer Concentrated Non-Overlapping Winding

An advantage of a single layer concentrated windings is simpler automatized winding process and better fault tolerance compared to their double layer counterparts. They use every other tooth for winding which results in the simpler automatized winding. The better fault tolerance comes with better physical and electrical separation between coil turns. Although the benefits with this winding looks attractive, the double layer windings are actually more common today. It is mostly because single layer winding suffers from longer end windings and higher inductance.

Chapter 5

Operating principle and equivalent circuits

5.1 Operating Principle

In the majority of designs the rotating assembly in the center of the generator the "rotor" contains the magnet, and the "stator" is the stationary armature that is electrically connected to a load. A set of three conductors make up the armature winding in standard utility equipment, constituting three phases of a power circuit that correspond to the three wires we are accustomed to see on transmission lines. The phases are wound such that they are 120 degrees apart spatially on the stator, providing for a uniform force or torque on the generator rotor. The uniformity of the torque arises because the magnetic fields resulting from the induced currents in the three conductors of the armature winding combine spatially in such a way as to resemble the magnetic field of a single, rotating magnet. This stator magnetic field or "stator field" appears as a steady rotating field and spins at the same frequency as the rotor when the rotor contains a single dipole magnetic field. The two fields move in "synchronicity" and maintain a fixed position relative to each other as they spin. [44] They are known as synchronous generators because f, the frequency of the induced voltage in the stator (armature conductors) conventionally measured in hertz, is directly proportional to RPM, the rotation rate of the rotor usually given in revolutions per minute (or angular speed). If the rotor windings are arranged in such a way as to produce the effect of more than two magnetic poles, then each physical revolution of the rotor results in more magnetic poles moving past the armature windings. Each passing of a north and south pole corresponds to a complete "cycle" of a magnet field oscillation. Therefore, the constant of proportionality is, where P is the number of magnetic rotor poles (almost always an even number), and the factor of 120 comes from 60 seconds per minute and two poles in a single magnet.

$$f\,(\mathrm{Hz}) = RPM\frac{\mathrm{P}}{120}$$

In a permanent magnet generator, the magnetic field of the rotor is produced by permanent magnets. Other types of generator use electromagnets to produce a magnetic field in a rotor winding. The direct current in the rotor field winding is fed through a slip-ring assembly or provided by a brushless exciter on the same shaft

5.2 Equivalent circuit

Permanent magnet generators do not require a DC supply for the excitation circuit, nor do they have slip rings and contact brushes. However, large permanent magnets are costly which restricts the economic rating of the machine. The flux density of high performance permanent magnets is limited. The air gap flux is not controllable, so the voltage of the machine cannot be easily regulated. A persistent magnetic field imposes safety issues during assembly, field service or repair. High performance permanent magnets, themselves, have structural and thermal issues. Torque current MMF vector ally combines with the persistent flux of permanent magnets, which leads to higher air-gap flux density and eventually, core saturation. In this permanent magnet alternators the speed is directly proportional to the output voltage of the alternator

Similarly as separately excited synchronous machines, the PM synchronous machines are usually treated in a dq reference frame fixed to the rotor, Figure 3.1. The equivalent circuit of the machine is almost the same as for a separately excited synchronous machine.

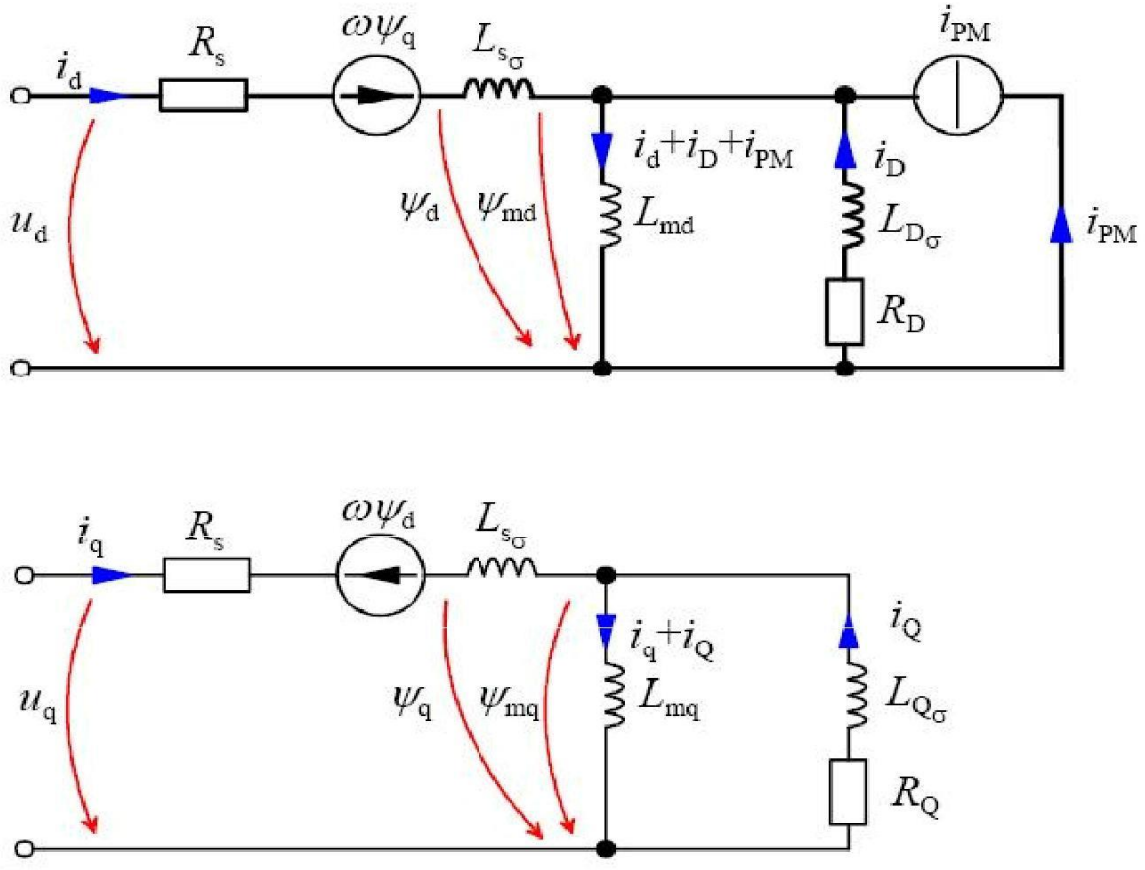

Figure 5.1 Equivalent circuit of PMSG on rotor reference [52]

5.3 Equivalent circuit equations

Figure 5.1 Equivalent circuits of a PMSM in the d- and q-directions. The permanent magnet can be depicted by a current source *i*PM in the rotor circuit; in the magnetizing inductance, this current source produces the permanent magnet's share of the air gap flux linkage.

PM = *i*PM *L*md

If also the damper windings are included in the model, the voltage equations of a PM machine differ from a separately excited synchronous machine only by the fact that the equation for the field winding is lacking. Thus, the voltage equations of the PM machine are given in the rotor reference frame in the familiar form

The flux linkage components in the equations are determined by the equations

$$u_{sd} = R_s i_{sd} + \frac{d\psi_{sd}}{dt} - \omega\psi_{sq}, \quad (5.1)$$

$$u_{sq} = R_s i_{sq} + \frac{d\psi_{sq}}{dt} + \omega\psi_{sd}, \quad (5.2)$$

$$0 = R_D i_D + \frac{d\psi_D}{dt}, \quad (5.3)$$

$$0 = R_Q i_Q + \frac{d\psi_Q}{dt}. \quad (5.4)$$

The flux linkage components in the equations are determined by the equations

$$\psi_{sd} = L_{sd} i_{sd} + L_{md} i_D + \psi_{PM}; \quad (5.5)$$

$$\psi_{sq} = L_{sq} i_{sq} + L_{mq} i_Q, \quad (5.6)$$

$$\psi_D = L_{md} i_{sd} + L_D i_D + \psi_{PM}, \quad (5.7)$$

$$\psi_Q = L_{mq} i_{sq} + L_Q i_Q. \quad (5.8)$$

(5.9)

The flux linkage of the permanent magnet can be considered to be generated by the field current

$$i_{\mathrm{PM}} = \frac{\psi_{\mathrm{PM}}}{L_{\mathrm{md}}} \tag{5.10}$$

Chapter 6

Thermal Behavior and Cooling System

There are different sources of losses in electrical machines i.e. iron losses, copper losses, etc. The losses give rise to temperature, which has dramatic influence on performance and lifetime of electrical machines. Hence, study of thermal behavior of an electrical machine is vital. The temperature rise in the machine is strongly dependent on the load. In wind systems, the speed and the torque are very often lower compared with the ratings of the machine and varies with the wind conditions. The advantage is that the average temperature rise will be lower in comparison to the rated operating point. However, in order to guarantee high performance and long lifetime in any operation condition, the thermal calculations are performed based on the rated operation. In the following subsections, consequences of temperature rise are presented and different cooling systems are discussed. A brief introduction to heat transfer theory is given, while more detailed theory is left for the reader. The most emphasis is put on introduction of sources of losses in the last subsection.

6.1 Consequences of Temperature Rise Performance

Thermal loading determines pretty much the power rating of the electrical machine. Values such as current density are often limited to a certain value depending on the cooling conditions in an electrical machine. This bounds current loading and respectively torque rating of the electrical machine. In other words, even if it is possible to manufacture more compact machines with higher torque densities, cooling capability restricts further reduction in the size.

The lifetime of an electrical machine is also affected by the so called thermal ageing, which influences the insulation. One of the requirements on winding insulation is to transfer the heat and to tolerate thermal stresses during normal and faulty conditions. Commercially available insulation material can tolerate limited temperature rise

Acceptable lifetime is expected, if the insulation material working temperature conforms to above conditions. On the other hand, due to an empirical law, lifetime of an insulation material halves with every 10 *K* extra temperature rise above the nominal

Temperature. Temperature influences magnet characteristics and it can increase risk of demagnetization. Figure 6.1 shows B-H curve of a typical PM material for different temperatures. The coercivity and remanence flux density decrease when the temperature increases. The knee point also moves upwards. The working point shifts on working line of the magnetic circuit downwards when the temperature increases. Given a high enough temperature and an improperly designed magnetic circuit, the working point will drop below the knee point, where the magnet loses its magnetic properties. If the machine is to be run again, PM has to be remagnetised, which is a complicated and tedious task.

Table 6.1

Insulation Class	**Hot Spot Temperature in ◦*C***
A	105
E	120
B	130
F	155
H	80

Different classes of an insulation material due to *IEC* −85.[56]

Overload increases the risk of demagnetisation. In these conditions the temperature exceeds the rated value and the remanence flux density of magnet decreases. If the magnetic circuit is not properly designed, PM magnetic flux will reduce remarkably. In order to compensate the reduction of the magnetic flux, the control unit will tend to increase the current in the stator winding, since the load torque should be kept the same. As a result, copper losses in the windings are increased and the temperature raises more in the windings and eventually in the magnets. This leads to even higher reduction of remanence flux density. In theory, reoccurrence of this cycle can eventually lead to demagnetisation of the magnets.

However, in order to avoid demagnetisation during overload conditions, protection equipment against Over-temperature condition is offered. Among PMSGs, Inset magnet machines and SMPMs are more vulnerable and are at a greater risk of demagnetisation compared to their IPM counterpart. Iron bridges around the magnets in IPMs saturate during faulty conditions and they counteract penetration of strong reverse field into the magnets. However, the temperature rise can still be high, because the magnets are buried and the cooling of magnets is more difficult.

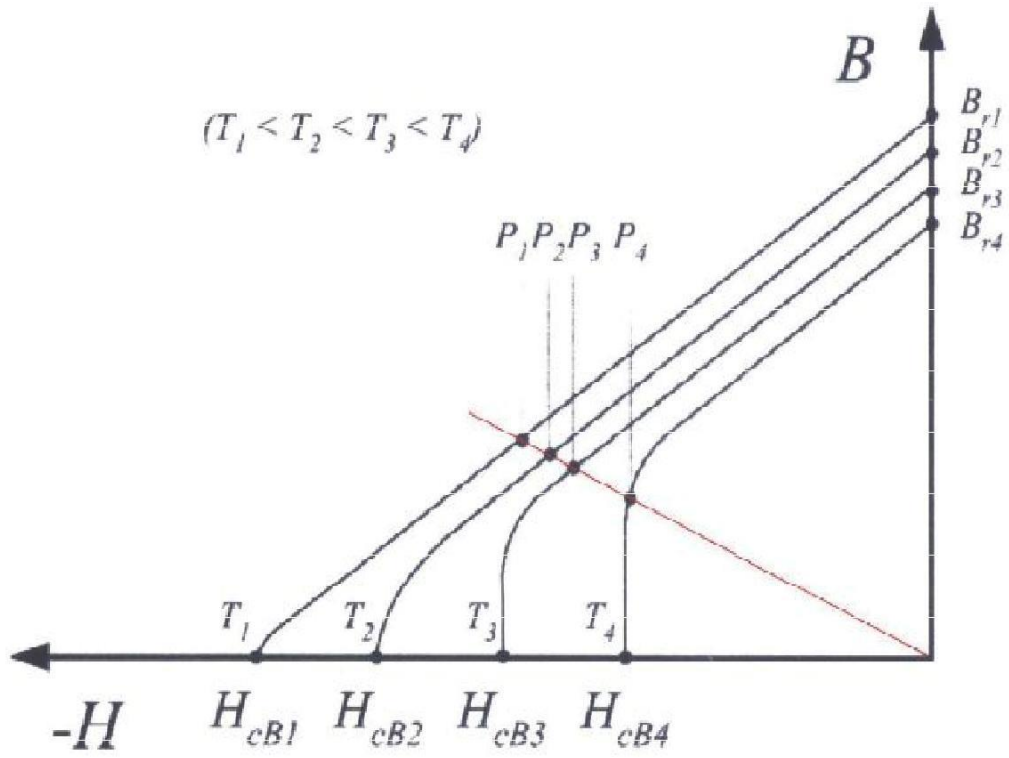

Figure 6.1 A typical magnet characteristics curve [34].

6.2 Cooling System

Cooling system facilitates dissipation of the heat, which will reduce temperature rise in the machine. Usually electrical machines are forced cooled by air or water. In air cooled machines a fan forces the air along the airgap. In water cooled machines the pump forces the water through tubes that are located in ducts. There are different possibilities for putting the ducts inside the machine, they can be located axially or spirally. Moreover, they can be located within the mantel (frame) or in the stator core. Putting ducts in stator core provides

better heat transfer, however, it influences the manufacturing process of the stator laminations. Kylander has developed an analytical model for thermal analysis of induction machines based on experimental results [11]. The model introduces thermal resistances. Lindström has developed a thermal model for a PMSG [11].

6.3 Heat Transfer Theory

Heat transfer is a result of a difference in the temperature. The heat is always transferred from higher temperature towards the lower temperature. It occurs in three different forms namely conduction, convection and radiation.

6.3.1 Conduction

Heat transfer through a substance is defined as conduction. The substance can be in any state: gas, liquid or solid. To measure conductive property of a material thermal conductivity is introduced. Usually the value of the thermal conductivity of materials lies in the range between 0.026 *W/m/K* for air and 427 *W/m/K* for silver [13]. Conduction is modeled by Fourier's law which also can be applied when heat is generated inside the body. However, when the time variation of conduction is considered, specific heat capacity of the body, which represents thermal capacity, is also introduced. In steady state analysis, however, this is neglected. In the field of electrical machines, conduction is the most common form of heat transfer in both steady state and transient conditions.

6.3.2 Convection

Heat transfer from a heat source by means of fluid movement is defined as convection. Fluid flow is caused by an external force either in natural or in forced conditions. In the former, discrepancy in fluid density creates the force; In the latter the force is caused by a pump or a fan. To measure convective property of a fluid, heat transfer coefficient is introduced. Average heat transfer coefficient of a fluid lies in a range between 6 *W/m2/K* for natural air convection and 120, 000 *W/m2/K* for condensing of steam [13]. Estimation of this value is complicated, since it depends on many variables like geometry of the surface, temperature difference, flow mechanical characteristics and physical characteristics of fluid i.e. viscosity.

Convection is explained by Newton's law of cooling. In the field of electrical machines, convection is the second most common form of the heat transfer in the steady state, but it does not play a remarkable role in transient conditions.

6.3.3 Radiation

Heat transfer by means of radiation does not need any substance. Thermal radiation is a function of couple of parameters as reflectivity, temperature difference, emissivity and geometry. It is modeled by Stefan Boltzman's law. In electrical machines the amount of radiation is negligible.

Chapter 7

Losses in PMSG

The main function of an electrical generator is to convert energy from mechanical into electrical. However, a part of energy is lost during this process which is referred to as losses. In electrical machines losses are divided into two categories i.e. normal losses and stray losses. Stray losses are additional losses that arise in an electrical machine aside from the normal losses considered in usual performance calculations for motor efficiency [15]. The main part of the stray losses is usually caused by eddy currents due to the leakage flux.
The normal losses involve copper losses in stator windings, iron losses in stator and mechanical losses such as friction. The iron and the copper losses are the biggest contributors to the losses in PMSG. One advantage of PMSG over IG is elimination of the copper losses in the rotor, namely slip loss [14]. Estimation of normal losses is easy and the corresponding knowledge is well established. On the other hand estimation of stray losses is complicated as they depend on many parameters. This complication might lead to inaccuracy in the calculations of the thermal behavior of the machine. A thorough discussion of losses is presented in order to improve a better perspective over variety of origins of losses.

7.1 Stator Core Losses

Various phenomena associated with variation of magnetic flux results in the stator core losses. Among them, the rotational and excess losses are probably less well known while the hysteresis and eddy current are more familiar. Here, hysteresis and eddy currents losses are introduced first together with Epstein frame test. Then, the two former are presented. Finally counteractive measures are suggested. Eddy currents are induced in the stator iron due to variation of magnetic field based on the Faraday's Law and they create losses based on the Ohm's Law. The amount of losses depends on the time rate of change of magnetic flux density. Assuming sinusoidal variation of magnetic flux density, eddy currents loss will depend on electric properties of material as well as applied field, including frequency and maximum value of magnetic flux density. Hysteresis losses are caused by magnetic properties of ferromagnetic material in a time varying magnetic field. The amount of these

Losses depends mostly on the magnetic properties of the material but also on the applied field, including its frequency and maximum value of magnetic flux density.
To estimate the iron losses in the stator, the results from Epstein frame test are used in analytical calculation. Accurate prediction of iron losses is much more difficult in comparison to copper losses. Accordingly, steel manufacturers provide the machine designer with results from the Epstein frame test. In this test the iron losses of steel material, subjected to various magnetic flux densities (in terms of amplitude and frequency) are measured. Simplified analytical models are developed to estimate the iron losses in electrical machines based on the results of Epstein frame test. These analytical methods are validated by means of comparison to experiments on similar machines or FEM simulations. Angular direction of magnetic field is, usually, constant in the stator. But it varies in regions of stator where the teeth and the yoke are connected to each other. This results in rotational loss. In the region where it exists, it adds to the core losses. Excess loss is not a well-known phenomenon. In order to include the effect of rotational and excess losses, the value of estimated core losses is, usually, multiplied by a correction factor.
Calculated results of core losses may differ from the experimental results for a number of reasons. Applied field in the machine is assumed to be uniformly sinusoidal in different physical points and the magnetic properties of the material are assumed to be uniform. However, in real machines these conditions are not prevailing perfectly. A waveform of the magnetic flux density is non sinusoidal and non-uniform. Influence of harmonics, which results in non-sinusoidal magnetic flux density, on the core losses will be introduced later in the text. Furthermore, the magnetic property of material varies when it is subjected to mechanical stresses during manufacturing e.g. punching. There are various solutions available in order to reduce the core losses. Some more common are laminated core with thin iron lamination, high resistivity and alloyed contents like silicon. These measures reduce eddy current losses. Another solution in order to reduce the iron losses is to reduce nominal frequency. However, the frequency is proportional to the rotor speed and to the number of poles. As the rotor speed is determined by the application, the frequency, therefore, cannot be chosen arbitrarily. Furthermore, increasing the number of poles reduces the pole pitch which in practice cannot be chosen too short. Laminations are annealed after they are stamped or cut, in order to compensate the manufacturing stresses. Variation of magnetic characteristics in cut edges is then avoided.

7.2 Mechanical Losses

Mechanical losses are relatively small in comparison to other losses especially in low speed applications. It encompasses two parts, namely windage and bearing. Windage losses are caused by mechanical friction of air and rotor surface. It depends on various parameters and phenomena and it is quite complicated to calculate more accurately. For instance it depends on gas properties and the prevailing gas flow characteristics. In electrical machines the gas flow is mostly turbulent in high speed applications and it is laminar in low speed application. An experimental equation in [15] gives a rough estimate of windage loss.

$$P_{windage} = C_f \rho \pi \omega_m^3 R^4 L \tag{7.1}$$

Where ℓis the mass density of the gas, ώ*m* is the mechanical angular speed of rotor and *R* and *L* are radius and length of the airgap cylinder respectively. *Cf* is the friction coefficient which is empirically determined. Mechanical loss in the bearings depends on parameters like bearing type, lubricator physical characteristics, shaft mechanical load and rotor speed, where lubricator characteristics are dependent on the temperature. An experimental equation in [15] gives a rough estimate of bearing loss.

$$P_{bearing} = C_b D_m^3 \omega_m \tag{7.2}$$

Dm is the average diameter of bearing and *Cb* is the bearing coefficient, which again is an empirical factor.

7.3 Stray Losses

Stray losses are divided into stray no-load losses and stray load losses. Generally, the former is represented by permeance variation and the latter is represented by leakage flux. Space harmonics' origin is due to the non-sinusoidal distribution of windings, saliency and slotting effect in an electrical machine. Time harmonics are generated by power electronics converters operated with electrical machines. High frequency of parasitic effects results in induction of eddy current in metal parts. Active material of the machine like stator conductors, rotor core and rotor permanent magnets are prone to stray losses. In the following, stray losses are introduced based on the location of losses. First AC winding losses

are discussed, second stray losses in permanent magnets are described and finally stray losses in rotor core are mentioned.

7.3.1 Stator Winding

Eddy currents are induced in the stator windings in the form of skin and proximity effects. If the source of varying applied field is the winding itself, the phenomenon is called skin effect. If the source of varying applied field is an external origin like rotor magnets, the phenomenon is called proximity effect. Eddy currents originating from skin and proximity effects in machines will give rise to non-uniform current density distribution within the conductor, i.e. less concentration in the center and more concentration on the circumference. As a consequence, effective cross section area for the current will be lower compared with the available cross section. This leads to higher AC resistance and higher losses.

7.3.2 Permanent Magnets

Eddy currents losses can be induced in permanent magnets in certain conditions. As mentioned, certain slot pole number combinations in concentrated winding design will result in space harmonics. This influence is more pronounced in high speed machines with high frequency. F. Sahin in [35] suggests an analytical estimation of eddy current losses in permanent magnets. In order to reduce these losses a proposed solution is magnet segmentation. In general no load stray losses caused by permeance variation can be reduced by increasing the airgap length or by using magnetic wedges.

7.3.3 Rotor Iron

Eddy currents losses can be induced in rotor core in certain conditions. In absence of parasitic effects, the magnetic flux density in the rotor iron is constant. Harmonics, e.g. created by the slotting effect, distort magnetic flux in the rotor. However, in SMPM machines, effective airgap is large and these losses are insignificant [12]. Again these losses are more pronounced in high frequency machines, but it should be mentioned that a careful selection of slot pole number combination in concentrated winding is mandatory.

CHAPTER 8

Modeling of the whole system

8.1 Modeling of the system

A schematic diagram of the whole system is shown in Fig. 8.1, where V_w is the wind velocity, back-to-back full-scale converters are used, C is the dc (direct current) link capacitor, U_{dc} is the dc voltage, L is the equivalent filter inductance, U_k is the voltage phasor of gird-side converter.

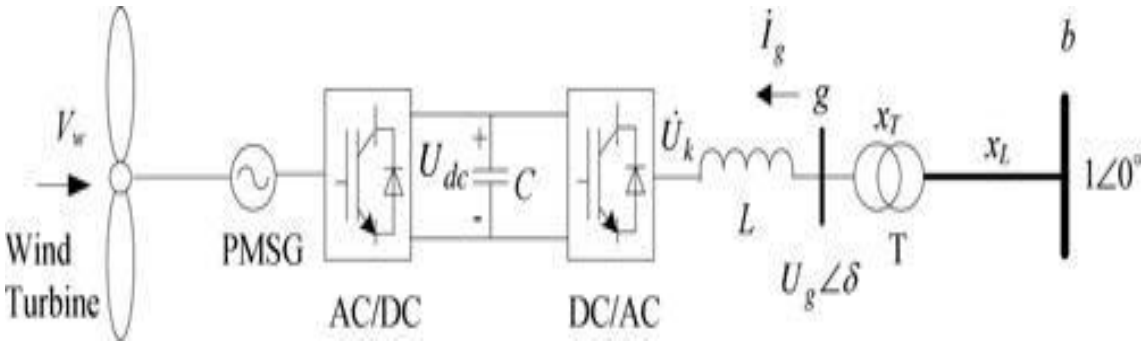

Fig 8.1: Schematic diagram of the whole system

$U_g < \delta$ is the voltage phasor of node g, $\dot{I}_g$ is current phasor, X_T is the reactance of transformer T, x_L is the reactance of transmission line, the voltage of power grid node bis $1 < 0^o$.

8.2 Modeling of the wind turbine

The equations of wind turbine are given by

$$T_w = 0.5 C_p \rho A V_w^3 / \Omega_w \tag{8.1}$$

$$C_p = 0.22\left(\frac{116}{\gamma_i} - 0.4\beta - 5\right)e^{-12.5/\gamma_i} \tag{8.2}$$

$$\frac{1}{\gamma_i} = \frac{1}{\gamma_i + 0.08\beta^2} - \frac{0.035}{\beta^3 + 1} \tag{8.3}$$

Where V_w is the wind velocity, ρ is the air density, A is the area of the blade, $A=\pi R^2 R_w$ is the radius of blade, Ω_w is the rotational velocity of the wind turbine, C_p is the utilization coefficient of wind power, which is related with tip velocity
Ratio λ ($\lambda= \Omega_w R_w / V_w$) and pitch angle β. When the wind turbine operates under the rated wind velocity, pitch angle β is set at an optimal value that allows the turbine to extract maximum energy from incident wind [15]. When wind velocity exceeds rated, pitch controller is used to obtain constant power. But taking into account the delay in mechanical actuator, only pitch controller is not sufficient to obtain constant power when a wind gust happens. Hence reference [24] brought up a strategy that pitch controller and generator power controller coordinate with each other, and the generator's power is limited to rate by setting the electro- magnetic torque reference according to the rated power and real-time rotational velocity.
In view of the focus of this paper, only the condition when wind velocity under the rated was considered, and pitch angle is kept constant at $\beta=0^o$, which does not influence the small-signal modelling and analysis.

8.3 Modeling of the PMSG
When the direction ofd-axis is aligned with rotor's magnetic flux linkage, the equations of PMSG can be given by (4) and (5), and the vector diagram is shown in Fig 8.2.

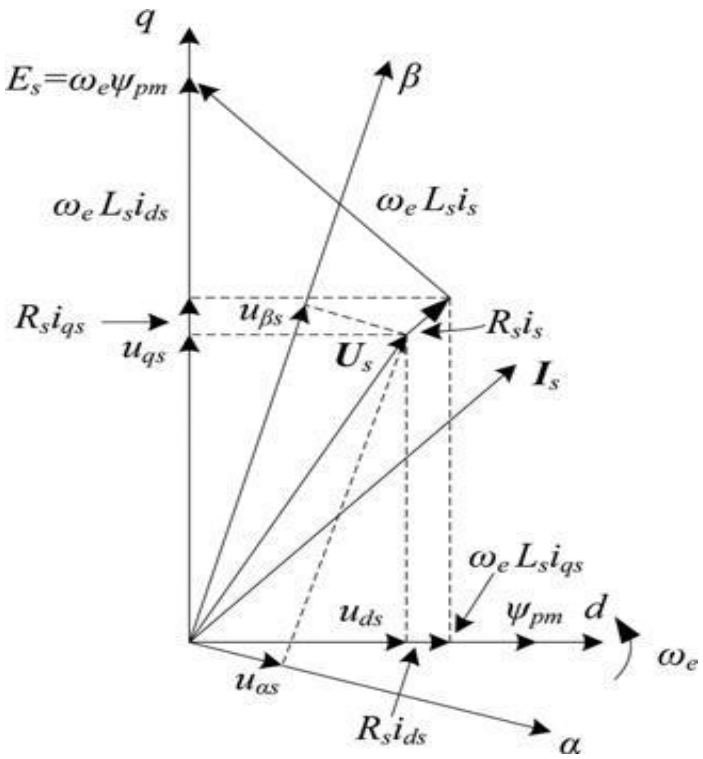

Fig 8.2: Vector diagram of PMSG in αβ and dq reference frame

$$u_{ds} = -R_s i_{ds} + \omega_e L_s i_{qs} - L_s \frac{di_{ds}}{dt}$$
$$u_{qs} = -R_s i_{qs} + \omega_e L_s i_{ds} - L_s \frac{di_{qs}}{dt} + \omega_e \Psi_{pm} \quad (8.4)$$

$$T_e = \frac{3}{2} n_p \Psi_{pm} i_{qs} \quad (8.5)$$

Where ω_e is the electrical angular velocity of generator, $\omega_e = n_p \Omega$, n_p is the number of poles, Vis the mechanical angular velocity of generator, $\Omega = \Omega_w$. ψ_{pm} is the rotor's magnetic flux linkage.

8.4 Modeling of the drive train

The rotors of wind turbine and the generator are connected directly, so they can be expressed together by

$$\frac{d\Omega}{dt} = \frac{1}{\tau_j}(T_w - T_e) \quad (8.6)$$

Where $\tau_j$the equivalent inertia is time constant of the whole drive train.

8.5 Modeling of converters and their controllers

8.5.1 Equations of generator-side controller

d-axis stator current i_{ds} is controlled to be zero, and q-axis stator current i_{qs} is controlled to to be zero, and q-axis stator current i_{qs} is controlled to track the maximal input of the wind turbine torque. The schematic diagram of generator side controller is shown in Fig.8.3

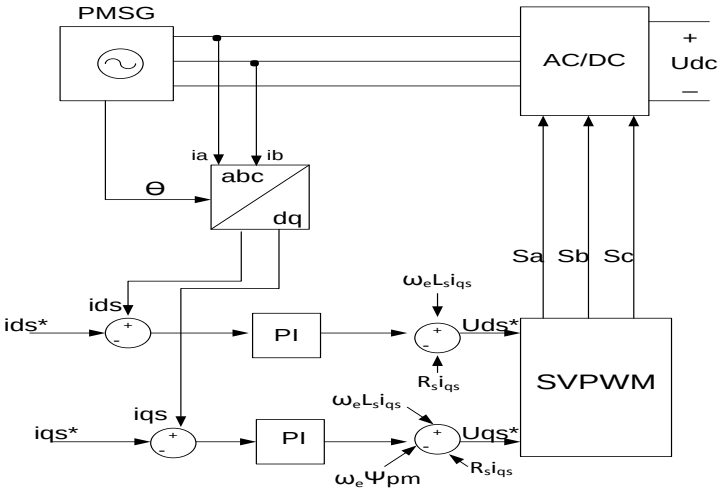

Fig 8. 3: Schematic diagram of generator-side controller

The equations of generator-side controller are given by

$$i^*_{ds} = 0$$

$$\frac{d\varphi_1}{dt} = i^*_{ds} - i_{ds}$$

$$u^*_{ds} = -K_{P1}(i^*_{ds} - i_{ds}) - K_{I1}\varphi_1 + \omega_e L_s i_{qs} - R_s i_{ds}$$

$$i^*_{qs} = \frac{2T^*_e}{3n_p\Psi_{pm}}$$

$$T^*_e = \frac{1}{2}C_{pmax}\rho\pi R^3_w V^2_w/\gamma_{opt}$$

$$\frac{d\varphi_2}{dt} = i^*_{qs} - i_{qs}$$

$$u^*_{qs} = -K_{P2}\left(i^*_{qs} - i_{qs}\right) - K_{I2}\varphi_2 + \omega_e L_s i_{ds} - R_s i_{qs} \qquad (8.7)$$

Where intermediate state variablesφ_1, φ_2 are introduced. Since the dynamic process of converter is much faster than electromagnetic and mechanical dynamic process, the dynamic process of converter can be ignored, so
$u_{ds} = u_{ds}^*, u_{qs} = u_{qs}^*$. According to the above equations

$$L_s \frac{di_{ds}}{dt} = K_{P1}(i_{ds}^* - i_{ds}) + K_{I1}\varphi_1$$

$$L_s \frac{di_{qs}}{dt} = K_{P2}\left(i_{qs}^* - i_{qs}\right) + K_{I2}\varphi_2 \quad (8.8)$$

8.5.2 Equations of grid-side converter and its controller

DQ-axis of grid side is used to distinguish dq axis of generator side here. When the direction of Q-axis is aligned with the voltage vector U_g , u_{Dg}=0, P_g=$u_{Qg}i_{Qg}$, Q_g=$u_{Qg}i_{Dg}$. The vector diagram of grid-side converter is shown inFig. 8.4.

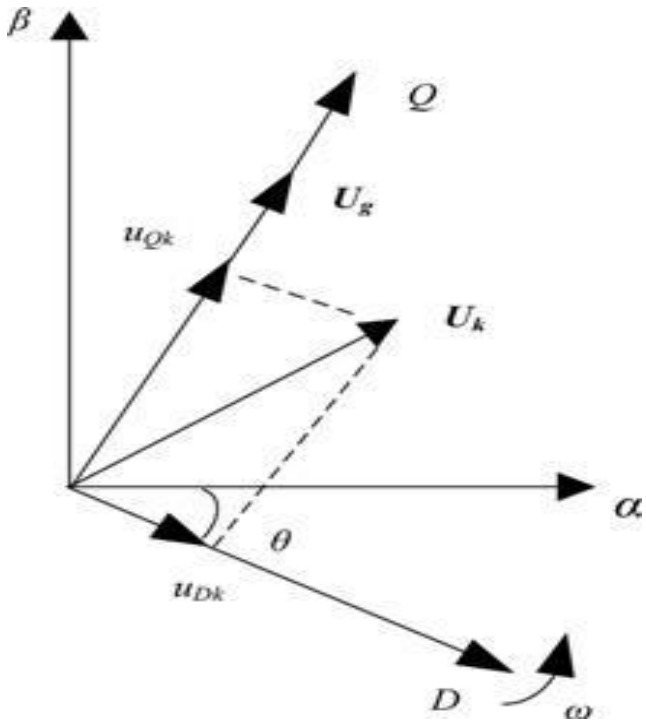

Fig.8. 4: Vector diagram of grid-side converter in αβ and dq reference frame

The equations of grid-side voltage source converter are given by

$$u_{Dk} = u_{Dg} - L\frac{di_{Dg}}{dt} + \omega L i_{Qg}$$
$$u_{Dk} = u_{Qg} - L\frac{di_{Qg}}{dt} + \omega L i_{Dg} \quad (8.9)$$

Where ω is the electrical angular velocity of power grid voltage.

D-axis stator current i_{Dg} is controlled to zero to obtain zero reactive power Q_g,
Q-axis stator current i_{Qg} is controlled to keep stable dc voltage. The schematic diagram of generator side controller is shown inFig. 5.5, and the control equations of grid side are given by

$$i^*_{Dg} = 0$$
$$\frac{d\varphi_3}{dt} = i^*_{Dg} - i_{Dg}$$
$$u^*_{Dk} = -K_{P3}\left(i^*_{Dg} - i_{Dg}\right) - K_{I3}\varphi_3 + \omega L i_{Qg} + u_{Dg}$$
$$\frac{d\varphi_4}{dt} = U^*_{dc} - U_{dc}$$
$$i^*_{Qg} = K_{P4}(U^*_{dc} - U_{dc}) + K_{I4}\varphi_4$$
$$\frac{d\varphi_5}{dt} = i^*_{Qg} - i_{Qg}$$
$$u^*_{Qk} = -K_{P5}\left(i^*_{Qg} - i_{Qg}\right) - K_{I5}\varphi_5 + \omega L i_{Dg} + u_{Qg} \quad (8.10)$$

Where intermediate state variables$\varphi_3, \varphi_4, \varphi_5$ are introduced. The dynamic process of converter can be ignored, so $u_{Dk}=u^*_{Dk}$, $u_{Qk}=u^*_{Qk}$ .According to the above equations following equations can be derived

$$L\frac{di_{Dg}}{dt} = K_{P3}\left(i^*_{Dg} - i_{Dg}\right) + K_{I3}\varphi_3$$
$$L\frac{di_{Qg}}{dt} = K_{P5}\left(i^*_{Qg} - i_{Qg}\right) + K_{I5}\varphi_5 \quad (8.11)$$

8.5.3 Equations of direct current voltage

The equation of dc link part is given by

$$\frac{dU_{dc}}{dt} = \frac{3}{2CU_{dc}}\left(U_{ds}i_{ds} + U_{qs}i_{qs} + U_{Qg}i_{Qg}\right) \quad (5.12)$$

8.6 Modeling of power grid

As shown in Fig.8.1, PMSG is connected with power grid through transformer and transmission line. The equations of power grid are given by

$$i_{Qg} = -\frac{sin\delta_g}{x_{TL}}$$
$$i_{Qg} = -\frac{u_{Qg}-cos\delta_g}{x_{TL}} \quad (8.13)$$

Where $x_{TL}=x_L+x_T$.

8.7 Complete small signal modeling

To study the system stability after suffering a small disturbance of a wind velocity step-down and step-up and to effectively design the controllers' parameters, it is necessary to build the complete small-signal model of the system. Linearizing (1) – (11) around steady-state values, the linearization differential equations of the whole system can be obtained.

$$\frac{d\Delta x}{dt} = A\Delta x + B\Delta u \quad (8.14)$$

Where

x= [Ω i_{ds} i_{qs} ϕ_1 ϕ_2 ϕ_3 ϕ_4 ϕ_5 i_{dg} i_{qg} u_{dc}]
u= V_w

Genetic Algorithm

The genetic algorithm is a method for solving both constrained and unconstrained optimization problems that is based on natural selection, the process that drives biological evolution. The genetic algorithm repeatedly modifies a population of individual solutions. [65]

Methodology

Optimization problems

In a genetic algorithm, a population of candidate solutions (called individuals, creatures, or phenotypes) to an optimization problem is evolved toward better solutions. Each candidate solution has a set of properties (its chromosomes or genotype) which can be mutated and altered; traditionally, solutions are represented in binary as strings of 0s and 1s, but other encodings are also possible.

The evolution usually starts from a population of randomly generated individuals, and is an iterative process, with the population in each iteration called a generation. In each generation, the fitness of every individual in the population is evaluated; the fitness is usually the value of the objective function in the optimization problem being solved. The more fit individuals are stochastically selected from the current population, and each individual's genome is modified (recombined and possibly randomly mutated) to form a new generation. The new generation of candidate solutions is then used in the next iteration of the algorithm. Commonly, the algorithm terminates when either a maximum number of generations has been produced, or a satisfactory fitness level has been reached for the population.

Matrix are

$$A = \begin{bmatrix} a_{11} & 0 & a_{13} & 0 & 0 & 0 & 0 & 0 & 0 & 0 & 0 \\ 0 & a_{22} & 0 & a_{24} & 0 & 0 & 0 & 0 & 0 & 0 & 0 \\ 0 & 0 & a_{33} & 0 & a_{35} & 0 & 0 & 0 & 0 & 0 & 0 \\ 0 & a_{42} & 0 & 0 & 0 & 0 & 0 & 0 & 0 & 0 & 0 \\ 0 & 0 & a_{53} & 0 & 0 & 0 & 0 & 0 & 0 & 0 & 0 \\ 0 & 0 & 0 & 0 & 0 & 0 & 0 & 0 & a_{69} & 0 & 0 \\ 0 & 0 & 0 & 0 & 0 & 0 & 0 & 0 & 0 & 0 & a_{711} \\ 0 & 0 & 0 & 0 & 0 & 0 & a_{87} & 0 & 0 & a_{810} & a_{811} \\ 0 & 0 & 0 & 0 & 0 & a_{96} & 0 & 0 & a_{99} & 0 & 0 \\ 0 & 0 & 0 & 0 & 0 & 0 & a_{107} & a_{108} & 0 & a_{1010} & a_{1011} \\ a_{111} & a_{112} & a_{113} & a_{114} & a_{115} & 0 & 0 & 0 & a_{119} & a_{1110} & a_{1111} \end{bmatrix}$$

$B = [b_1 \quad b_2 \quad b_3 \quad b_4 \quad b_5 \quad b_6 \quad b_7 \quad b_8 \quad b_9 \quad b_{10} \quad b_{11}]$

A typical genetic algorithm requires:

- A genetic representation of the solution domain,
- A fitness function to evaluate the solution domain.

A standard representation of each candidate solution is as an array of bits. Arrays of other types and structures can be used in essentially the same way. The main property that makes these genetic

representations convenient is that their parts are easily aligned due to their fixed size, which facilitates simple crossover operations. Variable length representations may also be used, but crossover implementation is more complex in this case. Tree-like representations are explored in genetic programming and graph-form representations are explored in evolutionary programming; a mix of both linear chromosomes and trees is explored in gene expression programming.
Once the genetic representation and the fitness function are defined, a GA proceeds to initialize a population of solutions and then to improve it through repetitive application of the mutation, crossover, inversion and selection operators.
Where except Vw, Rw, tj and t, all the variables are converted into per unit, TB is the base value of torque, VB is the base value of mechanical angular velocity and tB is the base value of time.

8.8 Analysis of small-signal model

A studied case was used to analyze the stability of the system after suffering a small disturbance. In this case, a 1.5 MW, 690 V, 22 r/min (48 poles) PMSG was used. The value of dc link capacitor was 2000 mF. An L-filter was designed to limit harmonic current. A transformer (690/35000 V) was used for grid connection.

GA Test Initialization

The population size depends on the nature of the problem, but typically contains several hundreds or thousands of possible solutions. Often, the initial population is generated randomly, allowing the entire range of possible solutions (the search space). Occasionally, the solutions may be "seeded" in areas where optimal solutions are likely to be found.

Selection

During each successive generation, a proportion of the existing population is selected to breed a new generation. Individual solutions are selected through a fitness-based process, where fitter solutions (as measured by a fitness function) are typically more likely to be selected. Certain selection methods rate the fitness of each solution and preferentially select the best solutions. Other methods rate only a random sample of the population, as the former process may be very time-consuming.

The fitness function is defined over the genetic representation and measures the quality of the represented solution. The fitness function is always problem dependent. For instance, in the knapsack problem one wants to maximize the total value of objects that can be put in a knapsack of some fixed capacity. A representation of a solution might be an array of bits, where each bit represents a different object, and the value of the bit (0 or 1) represents whether or not the object is in the knapsack. Not every such representation is valid, as the size of objects may exceed the capacity of the knapsack. The fitness of the solution is the sum of values of all objects in the knapsack if the representation is valid, or 0 otherwise.

In some problems, it is hard or even impossible to define the fitness expression; in these cases, a simulation may be used to determine the fitness function value of a phenotype (e.g. computational fluid dynamics is used to determine the air resistance of a vehicle whose shape is encoded as the phenotype), or even interactive genetic algorithms are used.

Eigen values

```
  1.0e+02 *

-8.6496 + 0.0000i
-2.7871 + 0.0000i
-2.1564 + 0.0000i
-0.0019 + 0.0000i
 0.2661 + 0.0509i
 0.2661 - 0.0509i
-0.4671 + 0.0000i
-1.0636 + 0.9980i
-1.0636 - 0.9980i
-0.5318 + 0.3777i
-0.5318 - 0.3777i
```

Eigenvaluetraces

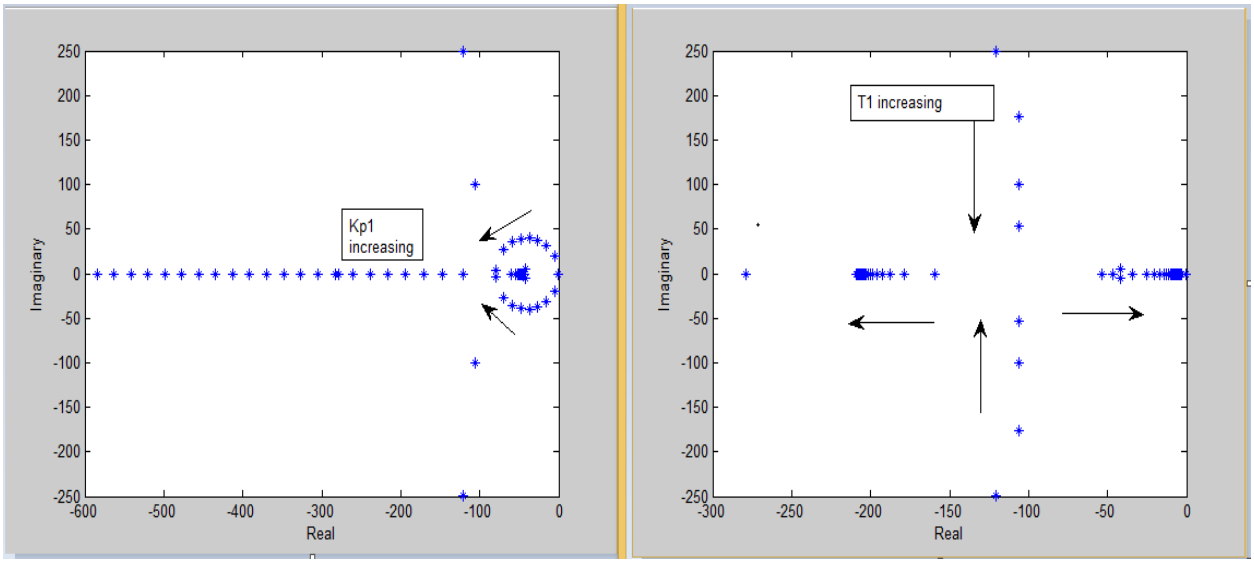

a and b

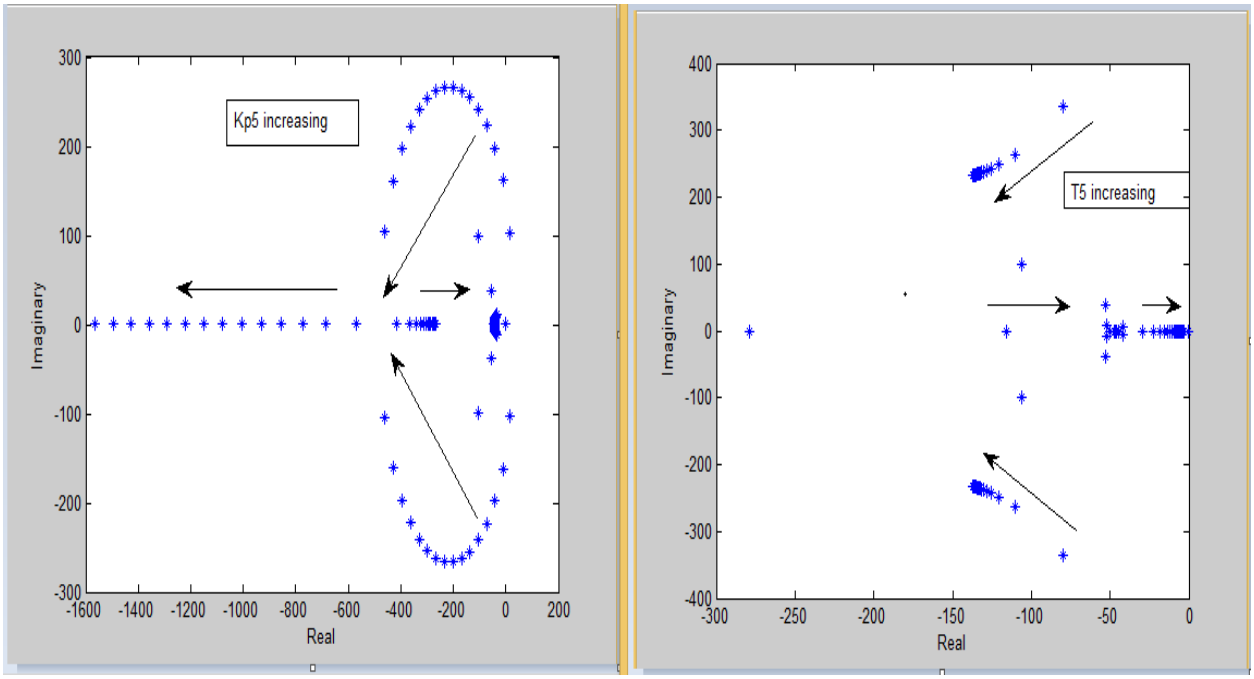

c and d

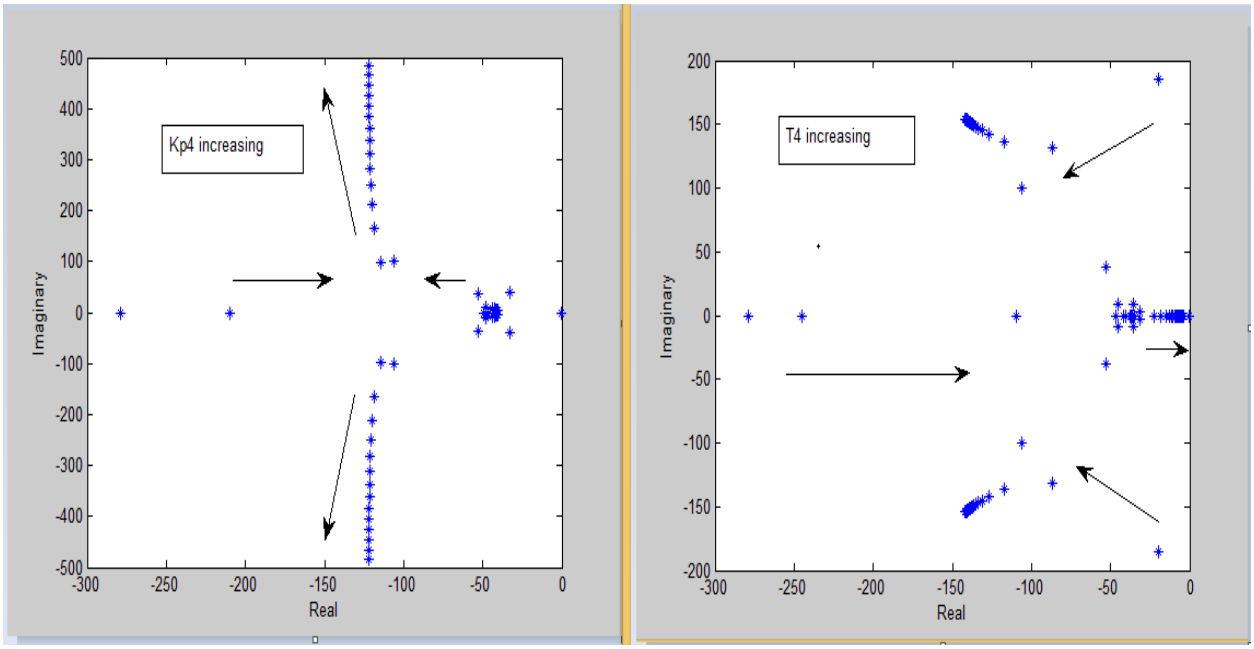

e and f

Fig. 8.5 Traces of eigenvalues as controllers' parameters are changed

a) $0.05 \leq KP1 \leq 3$, T1 ¼ 0.025
b) $0.005\ s \leq T1 \leq 0.3\ s$, KP1 ¼1
c) $0.05 \leq KP5 \leq 3$, T5 ¼ 0.025
d) $0.005\ s \leq T5 \leq 0.3\ s$, KP5 ¼0.5
e) $0.1 \leq KP4 \leq 1.5$, T4 ¼ 0.025
f) $0.005\ s \leq T4 \leq 0.3\ s$, KP4 ¼0.25

The eigenvalues of the state matrix A are calculated. It can be seen that the system is stable after suffering small disturbance because all of the eigenvalues have negative real parts. There are four oscillation modes and three evanescent modes. The participation factors can disclose the relation between the modes and the variables where all the participation factors are normalized into infinite norm.

As shown 3 are highly sensitive to w1 and ids, so they are mainly affected by KP1 and KI1. l4, 5 are highly sensitive to the state variables w2 and iqs (denoted by boldface in Table 3), so they are mainly affected by KP2 and KI2. 16 and l7 are highly sensitive to w3 and idg, so they are mainly affected by KP3 and KI3. l8, 9 and l10, 11 are highly sensitive to w4, w5, iqg and udc, so they are mainly affected by KP4, KI4, KP5 and KI5. 11 is associated with the V, but it is evanescent mode, so there is no electromechanical oscillation mode in this system.

In order to improve the dynamic performance of the system, proper controllers' parameters can be chosen according to the traces of eigenvalues. Let Ti ¼ KPi/KIi (i ¼ 1 – 6), the traces of eigenvalues as KPi and Ti are changed as shown in Fig. 8.5.

Fig. 8.5a shows the traces of eigenvalues as a function of KP1. It can been seen that as KP1 is changed, only l2,3 change, when KP1 is small, l2,3 are conjugated roots, as KP1 is increased, l2,3 move towards stable region and their imaginary parts increase first and then decrease and eventually become two evanescent modes, one moves towards stable region and one moves towards instable region. Fig. 8.5 b shows the traces of eigenvalues as a function of T1. It can been seen that as T1 is changed, only l2,3 change, when T1 is small, l2,3 are conjugated roots, as T1 is increased, their real parts are changeless, their imaginary parts decrease, and eventually they become two evanescent modes, one moves towards stable region and one moves towards instable region. It is can be analyzed that when KP1T1 ¼ 4TBLs, l2, 3 become two equal real roots and these equal real roots will be larger when T1 is smaller and KP1 is larger. The disturbance suppression is faster when the absolute value of the real part of the eigenvalues is greater. The oscillation frequency of the system is higher when the absolute value of the imaginary part of eigenvalue is larger. Taking into account the frequency of the inverter output voltage is 50 Hz, the oscillation frequency should be controlled in much less than 50 Hz, and the absolute value of the real part of eigenvalues should be taken as large as possible, so KP1 and T1 should be chosen to make l2, 3 be conjugated roots with large real part and small imaginary part.

As KP2 and T2 are changed, only l1 and l4, 5 change. l1 has a very little change and that do not have impact on system dynamic performance. The trace of l4, 5 are similar to Figs. 7a and b. The

choice of KP2 and T2 are similar to KP1 and T1, which will not be analyzed in detail here. As KP3 and T3 are changed, only l6, 7 change. The traces of l6, 7 are similar to Figs. 8.5 a and b, which will not also be analyzed in detail here.

KP5 and T5 are inner-loop parameters of grid controller. They are first analyzed here. Fig. 8.5 c shows the traces of eigenvalues as a function of KP5. It can been seen that as

KP5 is increased, l8, 9 and l10, 11 change. l8, 9 become from conjugated roots to two real roots. When KP5 is small, the real parts of l10, 11 are positive, the system is instable, as KP5 is increased, l10, 11 move from instable region to stable region, and become from conjugated roots to two real roots.

Fig. 7d shows the traces of eigenvalues as a function of T5. When T5 is small, l8, 9 are two real roots; as T5 is increased, l8, 9 become two conjugated roots, and their imaginary parts increase first and then decrease, their real parts decrease, and eventually they become two real roots again, and one moves towards stable region and one moves towards instable region. As T5 is increased, l10, 11 move towards stable region, and their imaginary parts decrease. So, KP5 and T5 should be chosen a middle value in Figs. 7c and d to make l8, 9 and l10, 11 be conjugated roots with large real part and small imaginary part. Fig. 8.5 e shows the traces of eigenvalues as a function of KP4. It can been seen that as KP4 is increased, l8, 9 and l10, 11 change. The real parts of l8, 9 decrease first and then increase, their imaginary parts decrease. When KP4 is small, l10, 11 are two real roots. As KP4 is increased, they become conjugated roots, and their real parts decrease, whereas their imaginary parts increase. Fig. 8.5 f shows the traces of eigenvalues as a function of T4. It can been seen that as T4 is increased, l8, 9 become from two evanescent modes to oscillation mode and finally to two evanescent modes. The real parts of l10, 11 decrease, whereas their imaginary parts decrease first and then increase. So, KP4 and T4 should be chosen a middle value in Figs. 7e and f. According to the above analysis, a set of reasonable parameters was chosen. KP1 ¼ 1 pu, T1 ¼ 0.018 s, KP2 ¼ 1, T2 ¼ 0.018 s, KP3 ¼ 1 pu, T3 ¼ 0.006 s, KP4 ¼ 0.25 pu, T4 ¼ 0.03 s, KP5 ¼ 0.5, T5 ¼ 0.02 s.

Genetic operators

Main articles are Crossover (genetic algorithm) and Mutation (genetic algorithm)

The next step is to generate a second generation population of solutions from those selected through a combination of genetic operators: crossover (also called recombination), and mutation.

For each new solution to be produced, a pair of "parent" solutions is selected for breeding from the pool selected previously. By producing a "child" solution using the above methods of crossover and mutation, a new solution is created which typically shares many of the characteristics of its "parents". New parents are selected for each new child, and the process continues until a new population of solutions of appropriate size is generated. Although reproduction methods that are based on the use of two parents are more "biology inspired", some research [43] [44] suggests that more than two "parents" generate higher quality chromosomes.

These processes ultimately result in the next generation population of chromosomes that is different from the initial generation. Generally the average fitness will have increased by this procedure for the population, since only the best organisms from the first generation are selected for breeding, along with a small proportion of less fit solutions. These less fit solutions ensure genetic diversity within the genetic pool of the parents and therefore ensure the genetic diversity of the subsequent generation of children.

Opinion is divided over the importance of crossover versus mutation. There are many references in Fogel (2006) that support the importance of mutation-based search.

Although crossover and mutation are known as the main genetic operators, it is possible to use other operators such as regrouping, colonization-extinction, or migration in genetic algorithms. [55]

It is worth tuning parameters such as the mutation probability, crossover probability and population size to find reasonable settings for the problem class being worked on. A very small mutation rate may lead to genetic drift (which is non-ergodic in nature). A recombination rate that is too high may lead to premature convergence of the genetic algorithm. A mutation rate that is too high may lead to loss of good solutions, unless elitist selection is employed.

8.9 Simulation results

A simulation model was built based on MATLAB/ SIMULINK to verify the correctness of small-signal model, as shown in Fig. 8.6. The switch frequency of IGBT Bridge was 10 kHz. The small disturbance was chosen to be a wind velocity step-down and step-up, and the simulation results are shown in Figs. 10 and 11, where the direction of iDg and iQg are opposite to Fig. 1. Since Pg ¼ uQg iQg, Qg ¼ uQgiDg, Figs. 10d, and e, 11d and e also indicate the dynamic responses of Pg and Qg. It can be seen that the system was stable after suffering a small disturbance of a wind velocity step-down and step-up.

When the system suffered a wind velocity step-up from 8 to 11 m/s at 1 s, according to (8.5), iqs should be controlled to increase from 0.45 to 0.85, Te should be controlled to increase from 0.47 to 0.89, as shown in Figs. 10b and c, iqs and and Te increased rapidly to set valve, and tend to be stable after several times oscillation. ids was controlled to zero, as shown in Fig. 10a.ids approached zero after several times oscillation. According to (10), iDg and iQg were controlled to obtain unit power factor output at node g, as shown in Figs. 10d and e, iDg was controlled to zero and iQg was controlled to Pg/uQg. In the control strategy of (10), when iQg increases, the current vector Ig will lead the voltage vector Ug, and this lead angle will increase first and then decrease; hence power factor in g will be negative, so iDg will be negative and increases first, then decreases, and comes near to zero at last, as shown in Fig. 10d. The dynamic process when the system suffered a wind velocity step-down was opposite to wind velocity step-up, which will not be described here

in detail.

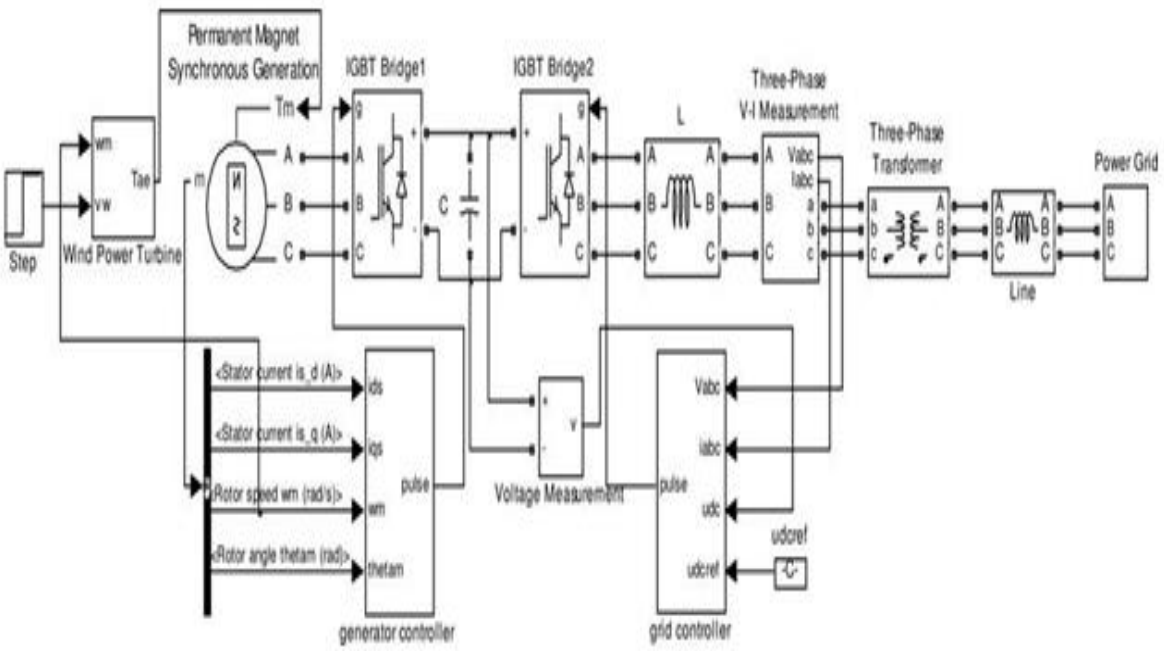

Fig: 8.6 Model of PMSG connected to power grid based on MATLAB/SIMULINK.

8.10 GA Test and Termination

This generational process is repeated until a termination condition has been reached. Common terminating conditions are:

- A solution is found that satisfies minimum criteria
- Fixed number of generations reached
- Allocated budget (computation time/money) reached
- The highest ranking solution's fitness is reaching or has reached a plateau such that successive iterations no longer produce better results
- Manual inspection
- Combinations of the above

Chromosome representation

The simplest algorithm represents each chromosome as a bit string. Typically, numeric parameters can be represented by integers, though it is possible to use floating point representations. The floating point representation is natural to evolution strategies and evolutionary programming. The notion of real-valued genetic algorithms has been offered but is really a misnomer because it does

not really represent the building block theory that was proposed by John Henry Holland in the 1970s. This theory is not without support though, based on theoretical and experimental results (see below). The basic algorithm performs crossover and mutation at the bit level. Other variants treat the chromosome as a list of numbers which are indexes into an instruction table, nodes in a linked list, hashes, objects, or any other imaginable data structure. Crossover and mutation are performed so as to respect data element boundaries. For most data types, specific variation operators can be designed. Different chromosomal data types seem to work better or worse for different specific problem domains.

When bit-string representations of integers are used, Gray coding is often employed. In this way, small changes in the integer can be readily affected through mutations or crossovers. This has been found to help prevent premature convergence at so called Hamming walls, in which too many simultaneous mutations (or crossover events) must occur in order to change the chromosome to a better solution.

Other approaches involve using arrays of real-valued numbers instead of bit strings to represent chromosomes. Results from the theory of schemata suggest that in general the smaller the alphabet, the better the performance, but it was initially surprising to researchers that good results were obtained from using real-valued chromosomes. This was explained as the set of real values in a finite population of chromosomes as forming a virtual alphabet (when selection and recombination are dominant) with a much lower cardinality than would be expected from a floating point representation. [69] [70]

An expansion of the Genetic Algorithm accessible problem domain can be obtained through more complex encoding of the solution pools by concatenating several types of heterogeneously encoded genes into one chromosome.[71] This particular approach allows for solving optimization problems that require vastly disparate definition domains for the problem parameters. For instance, in problems of cascaded controller tuning, the internal loop controller structure can belong to a conventional regulator of three parameters, whereas the external loop could implement a linguistic controller (such as a fuzzy system) which has an inherently different description. This particular form of encoding requires a specialized crossover mechanism that recombines the chromosome by section, and it is a useful tool for the modelling and simulation of complex adaptive systems, especially evolution processes.

Elitism

A practical variant of the general process of constructing a new population is to allow the best organism(s) from the current generation to carry over to the next, unaltered. This strategy is known as elitist selection and guarantees that the solution quality obtained by the GA will not decrease from one generation to the next. [72]

Parallel implementations

Parallel implementations of genetic algorithms come in two flavors. Coarse-grained parallel genetic algorithms assume a population on each of the computer nodes and migration of individuals among the nodes. Fine-grained parallel genetic algorithms assume an individual on each processor node which acts with neighboring individuals for selection and reproduction. Other variants, like genetic algorithms for online optimization problems, introduce time-dependence or noise in the fitness function.

Adaptive GAs

Genetic algorithms with adaptive parameters (adaptive genetic algorithms, AGAs) is another significant and promising variant of genetic algorithms. The probabilities of crossover (pc) and mutation (pm) greatly determine the degree of solution accuracy and the convergence speed that genetic algorithms can obtain. Instead of using fixed values of pc and pm, AGAs utilize the population information in each generation and adaptively adjust the pc and pm in order to maintain the population diversity as well as to sustain the convergence capacity. In AGA (adaptive genetic algorithm), [63] the adjustment of pc and pm depends on the fitness values of the solutions. In CAGA (clustering-based adaptive genetic algorithm), [74] through the use of clustering analysis to judge the optimization states of the population, the adjustment of pc and pm depends on these optimization states. It can be quite effective to combine GA with other optimization methods. GA tends to be quite good at finding generally good global solutions, but quite inefficient at finding the last few mutations to find the absolute optimum. Other techniques (such as simple hill climbing) are quite efficient at finding absolute optimum in a limited region. Alternating GA and hill climbing can improve the efficiency of GA while overcoming the lack of robustness of hill climbing.

This means that the rules of genetic variation may have a different meaning in the natural case. For instance – provided that steps are stored in consecutive order – crossing over may sum a number of steps from maternal DNA adding a number of steps from paternal DNA and so on. This is like adding vectors that more probably may follow a ridge in the phenotypic landscape. Thus, the efficiency of the process may be increased by many orders of magnitude. Moreover, the inversion operator has the opportunity to place steps in consecutive order or any other suitable order in favor of survival or efficiency. (See for instance [65] or example in travelling salesman problem, in particular the use of an edge recombination operator.)

A variation, where the population as a whole is evolved rather than its individual members, is known as gene pool recombination. A number of variations have been developed to attempt to improve performance of GAs on problems with a high degree of fitness epistasis, i.e. where the fitness of a solution consists of interacting subsets of its variables. Such algorithms aim to learn (before exploiting) these beneficial phenotypic interactions. As such, they are aligned with the Building Block Hypothesis in adaptively reducing disruptive recombination. Prominent examples of this approach include the mGA, [66] GEMGA [67] and LLGA. [68]

Chapter 9

Conclusion and future work

9.1 Models for stability studies

The main objective of our thesis is to find out the suitable values of control parameters to increase the performance of wind energy conversion process. After linearization, information regarding Eigen values and system parameters will be found. Through Eigen values characteristics the pole locations will be found that can define the system's overall performance stability. Stability of the system will be improved by adopting suitable values of control parameters.

Several Windings regarding generic models for the three wind turbine concepts for power system stability studies can be summarized as follows:

9.2 Fixed-speed wind turbine

A generalized model that can be used for deferent studies should include at least a two-mass drive train model and a third-order induction generator model with stator transient neglected. Only for a significantly large frequency 173 deviation, a modified fifth-order model needs to be used to provide more accurate responses.
Full power converter wind turbine: The generator was sufficiently modeled as a controlled electromagnetic torque with a time lag. The generator speed control by the generator-side converter must be represented, while the reactive control capability can be omitted. The dc-link capacitor and the dc-link voltage control were modeled in detail. The dc-link braking resistor was modeled as a negative power source controlled via a P-controller. If the dc-link capacitor is smaller than 0.02 pu, the dc-link model must be omitted from the model meaning that the grid-side converter power output is equivalent to the generator power output. The grid-side converter was modeled as a controlled current source. By adjusting the energy limit of the dc-link braking resistor, the model can resemble different FRT schemes of a PMSG. It was found that the drive train oscillations affect the grid-side converter output power. For all wind turbine concepts, the aerodynamic model should be represented as a

Cp lookup-table. This representation allows wind turbine operation with large speed variations and active stall or pitch control implementations.

The computational efficiency of the models was verified by the ability of the models to run in a simulation with a 10 ms integration time step using modified Euler solver.

Since no iteration is involved, the models can be conveniently implemented in a power system stability simulation tool. The accuracy of the models has been demonstrated by head-to-head comparisons against detailed models subjected to various disturbances.

The comparisons showed that responses of the proposed generic models match very well with those of the detailed models.

The wind turbine models proposed in this thesis can be seen as a contribution to the ongoing discourse on standardized models of wind power generation for power system stability studies. The generic models provide more opportunities for transmission system operators and wind farm developers to confidently perform system planning studies without being dependent on proprietary models and being restricted by non-disclosure agreements with manufactures.

9.3 Wind farm aggregated model

Aggregated models of wind farms consisting of large number of wind turbines were studied. It was found that a single equivalent unit representation of a wind farm is sufficient for most short-term voltage stability investigations. In case of a wind farm consisting of PMSG wind turbines or PMSGs, non-linearity due to MPT character-174 is tics and saturation of electrical controllers play no important role in characterizing wind farm responses provided that the active power control response is slow. This condition remains true even if power output discrepancies among the wind turbines in the wind farm are large. For a medium-term study, which may include wind transport phenomena, a cluster representation of a wind farm provides a more realistic prediction.

9.4 Dynamic reactive power compensation

Deferent influencing factors in designing dynamic reactive power compensation for an offshore wind farm consisting of fixed-speed wind turbines were investigated. The study found that FRT capability of the individual turbines in the wind farm utilizing an active stall control significantly reduces the requirement for the dynamic reactive power compensation. In the presented case, the reduction of the dynamic reactive power compensation requirement was more than 50% in comparison to the case when the wind turbines in the wind farm are not equipped with FRT

9.5 Future works

The following prospective topics, which are relevant to the current work, are proposed for future work more works need to be done to validate PMSG wind turbine and PMSG model presented in this thesis against field measurements data. The validations should comprise different operating conditions and fault types. It is interesting to simulate different wind turbine products available in the market using the proposed generic models. In some cases, it may need to derive and modify model parameters provided by manufacturers to adapt with the generic model representations. Technical and economic evaluations of various FRT schemes for wind farms. Study is needed to find the best FRT scheme options for different types of wind turbines and different grid requirements. More stringent grid codes have pushed wind turbines to include features similar to

those of conventional generators. This approach minimizes the negative impacts of wind turbines on the grid performance. On the other hand, the advancement of FACTS technology enables grid reinforcement in a cost effective way. It is therefore important to evaluate grid reinforcement by utilizing FACTS devices in comparison with improving wind turbine capability. Application of an HVDC for a large offshore wind farm is an interesting subject. A study is needed to investigate the influence of an HVDC on an increased stability of the wind farm and its potential to reduce wind turbine requirements. Investigation of impacts of different wind turbine concepts and capabilities on the stability of the Nordic power system 175 proposing a generalized approach for defining criteria for grid connections of wind farms taking into account characteristics and nature of the corresponding power system.

References

1. Steve Leone (25 August 2011). "U.N. Secretary-General: Renewables Can End Energy Poverty". Renewable Energy World.
2. "Offshore stations experience mean wind speeds at 80 m that are 90% greater than over land on average. Evaluation of global wind power "Overall, the researchers calculated winds at 80 meters [300 feet] above sea level traveled over the ocean at approximately 8.6 meters per second and at nearly 4.5 meters per second over land [20 and 10 miles per hour, respectively]." Global Wind Map Shows Best Wind Farm Locations. Retrieved 30 January 2006.
3. Worldwide energy society.
4. E. Hau. Wind turbines: fundamentals, technologies, application, economics. Springer Verlag Berlin Heidelberg, 2000.
5. J. Kjellin. Experimental vertical axis wind turbine system. PhD thesis, Uppsala University, Sweden, 2010.
6. S. Eriksson. Direct driven generators for vertical axis wind turbines. PhD thesis, Uppsala University, Sweden, 2008.
7. P. Deglair. Analytical aerodynamic simulation tools for vertical axis wind turbines. PhD thesis, Uppsala University, Sweden, 2010.
8. J.S. Linder, Small-Signal Model of the Parallel-Plane Vacuum Diode. Electronics Letters, 1965. 1(5): pp. 141-142.
9. F.A. Lindholm and P.R. Gray, Large-Signal and Small-Signal Models for Arbitrarily-Doped Four-Terminal Field-Effect Transistors. IEEE Transactions on Electron Devices, 1966. 13(12): pp. 819-829.
10. F.C. Fitchen, Limiting Amplitude for Mosfet Small-Signal Models. Proceedings of the IEEE, 1967. 55(12): pp. 2176-2177.
11. F. Lindholm, A. and D.J. hamilton, A Systematic Modeling Theory for Solid State Device. Solid State Electronics, 1964(7): pp. 171.
12. B. Choi, et al. Control Strategy for Multi-Module ParallelConverter System. Power Electronics Specialists Conference. 1990. pp. 225-234.
13. T. Kohama, et al. Dynamic Analysis of Parallel-Module Converter System with Current Balance Controllers. Telecommunications Energy Conference. 1994. pp. 190-195.
14. C. Byungcho, Comparative Study on Paralleling Schemes of Converter Modules for Distributed Power Applications. IEEE Transactions on Industrial Electronics, 1998. 45(2): pp. 194-199.
15. Y. Panov and M.M. Jovanovic, Stabilityand Dynamic Performance of CurrentSharing Control for Paralleled Voltage Regulator Modules. IEEE Transactions on Power Electronics, 2002. 17(2): pp. 172-179.
16. N. Pogaku, M. Prodanovic, and T.C. Green, Modeling, Analysis and Testing of Autonomous Operation of anInverter-Based Microgrid. IEEE Transactions on Power Electronics, 2007. 22(2): pp. 613-625.

17. Y. Li, D.M. Vilathgamuwa, and L. Poh Chiang, Design, Analysis, and Real-Time Testing of a Controller for Multibus Microgrid System. IEEE Transactions on Power Electronics, 2004. 19(5): pp. 1195-1204.
18. A. Tabesh and R. Iravani, Small-SignalModel and Dynamic Analysis of Variable Speed Induction Machine Wind Farms, in IET Renewable Power Generation. 2008. p. 215-227.
19. E.A.A. Coelho, P.C. Cortizo, and P.F.D. Garcia, Small-Signal Stability for Parallel-Connected Inverters in Stand-Alone Ac Supply Systems. IEEE Transactions on Industry Applications, 2002. 38(2): pp. 533-542.
20. A.L. Shenkman, B. Axelrod, and V.Chudnovsky, A New Simplified Model of the Dynamics of the Current-Fed Parallel Resonant Inverter. IEEE Transactions on Industrial Electronics, 2000. 47(2): pp. 282-286.
21. Myers, H. P., Introductory Solid State Physics, 2nd. Ed., Taylor & Francis, 1997.
22. Hellweg, Paul. The Insomniac's Dictionary. Facts On File Publications. p. 115. ISBN 0-8160-1364-0.
23. Brady, George Stuart; Clauser, Henry R; Vaccari, John A (2002). Materials Handbook: An Encyclopedia for Managers. McGraw-Hill Professional. p. 577. ISBN 0-07-136076-X.
24. Cullity, B. D.; C. D. Graham (2008). Introduction to Magnetic Materials. Wiley-IEEE. p. 485. ISBN 0-471-47741-9.
25. Arnold-Alnico Magnets. Arnoldmagnetics.com. Retrieved on 2011-07-30.
26. Hubert, Alex; Rudolf Schäfer (1998). Magnetic domains: the analysis of magnetic microstructures. Springer. p. 557. ISBN 3-540-64108-4.
27. "Standard Specifications for Permanent Magnet Materials (MMPA Standard No. 0100-00)" (PDF). Magnetic Materials Producers Association. Retrieved 9 September 2015.
28. Campbell, Peter (1996). Permanent magnet materials and their application. UK: Cambridge University Press. pp. 35–38. ISBN 0-521-56688-6.
29. "Evolution of Fe-Co rich particles in Alnico 8 alloy thermomagnetically treated at 800°C". Materials science and technology 16 (9): 1023–1028. 2000. doi:10.1179/026708300101508810.
30. Frequently Asked Questions. Magnetsales.com. Retrieved on 2011-07-30.
31. Carter, C. Barry; Norton, M. Grant (2007). Ceramic Materials: Science and Engineering. Springer. pp. 212–15. ISBN 0-387-46270-8.
32. Okamoto, A. (2009). "The Invention of Ferrites and Their Contribution to the Miniaturization of Radios". 2009 IEEE Globecom Workshops. pp. 1–42. doi:10.1109/GLOCOMW.2009.5360693. ISBN 978-1-4244-5626-0.
33. Shriver, D.F.; et al. (2006). Inorganic Chemistry. New York: W.H. Freeman. ISBN 0-7167-4878-9.
34. Ullah, Zaka; Atiq, Shahid; Naseem, Shahzad (2013). "Influence of Pb doping on structural, electrical and magnetic properties of Sr-hexaferrites". Journal of Alloys and Compounds 555: 263–267. doi:10.1016/j.jallcom.2012.12.061.
35. "Ferrite Permanent Magnets". Arnold Magnetic Technologies. Retrieved 18 January 2014.

36. Chemical Products Corporation. Retrieved 18 January 2014.
37. Hill Technical Sales. 2006. Retrieved 18 January 2014.
38. "Manufacturing Methods for Samarium Cobalt Magnets". Google Books. Defense Technical Information Center. Retrieved 18 May 2015.
39. Corrosion and oxidation resistance of Smco magnet, corrosion and oxidation resistance.
40. F. Magnussen. On design and analysis of synchronous permanent magnet machines for field weakening operation in hybrid electric vehicles. PhD thesis, Royal Inst. of Tech., Sweden, 2004.
41. F. Libert. Design, optimisation and comparison of permanent magnet motors for a low speed direct driven mixer. Lic. thesis, Royal Inst. of Tech., Sweden, 2004.
42. D. Svechkarenko. On design and analysis of a novel transverse flux generator for direct driven wind application. PhD thesis, Royal Inst. of Tech., Sweden, 2010.
43. L. H. Hansen et al. Conceptual survey of generators and power electronics for wind turbines. Technical report, Riso national lab, Roskilde, Denmark,
44. A. Grauers. Design of direct driven permanent magnet generators for wind turbines.PhD thesis, Chalmers Univ. of Tech., Sweden, 1996.
45. D. Svechkarenko. Thermal modeling and measurements of permanent magnet machines. Master's thesis, Royal Inst. of Tech., Sweden, 2004.
46. G. Kylander. Thermal modelling of small cage induction motors. PhD thesis, Chalmers Univ. Technol., Gothenburg, Sweden, 1995.
47. M. Degner A. Munoz, F. Liang. Evaluation of interior pm and surface pm synchronous machines with distributed and concentrated windings. In IECON, pages 1189–1193, 2008.
48. G. Kylander. Thermal modelling of small cage induction motors. PhD thesis, Chalmers Univ. Technol., Gothenburg, Sweden, 1995.
49. F. Magnussen. On design and analysis of synchronous permanent magnet machines for field weakening operation in hybrid electric vehicles. PhD thesis, Royal Inst. Of Tech., Sweden, 2004.
50. F. Libert. Design, optimisation and comparison of permanent magnet motors for a low speed direct driven mixer. Lic. thesis, Royal Inst. of Tech., Sweden, 2004.
51. D. Svechkarenko. On design and analysis of a novel transverse flux generator for direct driven wind application. PhD thesis, Royal Inst. of Tech., Sweden, 2010.
52. D. Hanselman. Brushless permanent magnet motor design. US: The Writer's Collective, 2 edition, 2003.
53. A. Grauers. Design of direct driven permanent magnet generators for wind turbines. PhD thesis, Chalmers Univ. of Tech., Sweden, 1996.
54. L. H. Hansen et al. Conceptual survey of generators and power electronics for wind turbines. Technical report, Riso national lab, Roskilde, Denmark,
55. N. Bainchi et al. Design considerations on fractional slot fault tolerant synchronous motors. In IEMDC, pages 902–909, 2005.
56. M. Degner A. Munoz, F. Liang. Evaluation of interior pm and surface pm synchronous machines with distributed and concentrated windings. In IECON, pages 1189–1193, 2008.

57. G. Kylander. Thermal modelling of small cage induction motors. PhD thesis, Chalmers Univ. Technol., Gothenburg, Sweden, 1995.
58. J. Lindström. Development of an experimental permanent magnet motor drive. Lic. thesis, Chalmers Univ. Technol., Gothenburg, Sweden, 1999.
59. D. Svechkarenko. Thermal modeling and measurements of permanent magnet machines. Master's thesis, Royal Inst. of Tech., Sweden, 2004.
60. R. Bonert C. Mi, G. R. Slemon. Modeling of iron losses of permanent magnet synchronous motors. In IEEE trans. on Inductrial Applications, volume 39, 2003.
61. F. Sahin. Design and development of a high speed axial flux permanent magnet machine. PhD thesis, Eindhoven Univ. of Tech., The Netherlands, 2001.
62. G. McPherson and R. D. Laramore. An Introduction to Electrical Machines and Transformers. Canada: John Wiley and Sons Inc, 2 edition, 1990.
63. L. H. Hansen A. D. Hansen. Market penetration of wind turbine concepts over the years. Technical report, Riso National Lab. Roskilde, Denmark, 2008.
64. N. Smith. Motors as Generators for Micro-Hydro Power. UK: Russel Press Ltd, 2 edition, 1997.
65. Eiben, A. E. et al (1994). "Genetic algorithms with multi-parent recombination". PPSN III: Proceedings of the International Conference on Evolutionary Computation. The Third Conference on Parallel Problem Solving from Nature: 78–87. ISBN 3-540-58484-6.
66. Taherdangkoo, Mohammad; Paziresh, Mahsa; Yazdi, Mehran; Bagheri, Mohammad Hadi (19 November 2012). "An efficient algorithm for function optimization: modified stem cells algorithm". Central European Journal of Engineering 3 (1): 36–50. doi:10.2478/s13531-012-0047-8.
67. Jump up^ Wolpert, D.H., Macready, W.G., 1995. No Free Lunch Theorems for Optimisation. Santa Fe Institute, SFI-TR-05-010, Santa Fe.
68. Jump up^ Goldberg, David E. (1991). "The theory of virtual alphabets". Parallel Problem Solving from Nature, Lecture Notes in Computer Science 496: 13–22. doi:10.1007/BFb0029726. Retrieved 2 July 2013.
69. Jump up^ Janikow, C. Z.; Michalewicz, Z. (1991). "An Experimental Comparison of Binary and Floating Point Representations in Genetic Algorithms" (PDF). Proceedings of the Fourth International Conference on Genetic Algorithms: 31–36. Retrieved 2 July 2013.
70. Jump up^ Patrascu, M.; Stancu, A.F.; Pop, F. (2014). "HELGA: a heterogeneous encoding lifelike genetic algorithm for population evolution modeling and simulation". Soft Computing 18: 2565–2576.
71. Jump up^ Baluja, Shumeet; Caruana, Rich (1995). Removing the genetics from the standard genetic algorithm (PDF). ICML.
72. Jump up^ Srinivas. M and Patnaik. L, "Adaptive probabilities of crossover and mutation in genetic algorithms," IEEE Transactions on System, Man and Cybernetics, vol.24, no.4, pp.656–667, 1994.

Appendix a

Abbreviations/full forms

B

BC= Before Christ.

BPDP= Bangladesh Power Development Board.

G

GEF= Global Environment Facility.

H

HAWT=Horizontal Axis Wind Turbines

L

LPF= Low Pass Filter.

P

PCF= Plant Capacity Factor.

PMSG= Permanent Magnet Synchronous Generator.

S

SM= Synchronous Machine.

U

UN= United Nations.

V

VAWT=Vertical Axis Wind Turbines.

VSM= Virtual Synchronous Machines.

W

WPD= Wind Power Density.

Appendix b

Symbols and their following meanings

A= Area of the blade.

$C_{p\,max}$ = Maximum utilization coefficient of wind power.

i_{ds} = d axis stator current.

i_{Dg} = D axis stator current.

i_{qs} = q Axis stator current.

K_{I1-I5} = Controller parameter.

K_{P1-P5}= Controller parameter.

L_s = Inductance of generator.

n_p= No. of poles.

R_w= Radius of blade.

U_{dc} = Direct current voltage.

U_{ds}= d axis stator voltage.

U_{qs}= q axis stator voltage.

$X_L + X_T$=X_{TL}= Power grid reactance.

Ω_w= Rotational velocity of wind turbine.

ψ_{pm}= Rotors magnetic flux linkage.

φ_{1-5}= Intermediate state variable.

ρ= Air density.

τ_j= Equivalent inertia time constant of the whole drive train.

V_w =Wind velocity.

γ= Tip velocity ratio.

γ_{opt} = Optimum value of Tip velocity ratio.